ISSN Number: 2454-2024(Online)

International Journal of Technical Research & Science

OPTIMAL CONTROL STRATEGY-BASED MULTILEVEL MATRIX CONVERTER FOR WIND POWER GENERATION SYSTEM

Kavita Sharma, Vinod Kumar
E-Mail Id: kavitasharmajoshi@gmail.com
Department of Electrical Engineering, College of Technology and Engineering, Maharana Pratap University of Agriculture and Technology, Udaipur, Rajasthan, India

Abstract- To test the performance of the control strategy through simulation under balanced and unbalanced situations, this work describes the creation of an optimal control strategy for performance enhancement in DFIG-based wind generation systems. To test the impacts under various input/output situations, a 2.2 KW multilevel matrix converter-based wind generation system prototype is built up in the lab. A DSpace DS1104 real-time board serves as the platform for the control system. It's important to research and develop wind turbine generator systems (WTGS) in order to produce a satisfactory output and efficient, high-quality power. With FLC, an ideal control plan is created and put into practice for performance improvement and efficiency optimization.

Keywords: Multilevel matrix converter, wind turbine emulator, wind energy conversion system (WECS), doubly fed induction generator (DFIG).

1. INTRODUCTION

Given the rising cost and declining quantity of fossil fuels like petrol and natural gas, renewable energy sources have emerged as essential for life. Wind energy has become one of the most promising sources of clean, green, and economical energy in recent years. Wind has a lengthy and exciting past. Around 5000 years ago, the Egyptians utilized wind for the first time and began to record it. Windmills were initially used to pump water in the Middle East. Then, it was estimated that more than 9000 small windmills have been used for a variety of purposes in Holland since the 1800s and that there are approximately six million in the US.

With a 1.25MW capacity and a 53-meter blade span, the largest wind turbine generator ever built in the US was installed in Grandpa's Knob, Vermont, in 1941. Construction of new fuel oil or natural gas-powered electric generation facilities was prohibited by policies and regulations like the National Energy Act. 56 of the 600 research projects reviewed by the Electric Power Research Survey (EPRI) in 1978 had a wind energy component. Second, the Power Plant Petroleum and Natural Gas Displacement Act of 1979 set a target of a 50% decrease in oil consumption. Additionally, it was anticipated that in 1980, utilities would complete roughly 100 wind projects. Following then, additional wind energy technology development and research also picked up speed.

The asymmetric heating of the atmosphere by the Sun, the rotation of the Earth, and the unevenness of the Earth's surface are all factors in the development of winds. Different Earth surfaces absorb the Sun's heat in various ways, and as a result, different winds are created. Over land, warm air rises and expands. Winds eventually form as heavier air rushes to fill the gap. Because air cools more quickly over water than it does over land during the day and at night, the wind changes direction. Managing intermittency is one technique to make wind energy more efficient because rotors run at different speeds depending on variations in wind speed. Efficiency is a further consideration; for maximum efficiency, the blade should move at a constant speed and with an absolute velocity equal to its relative speed.

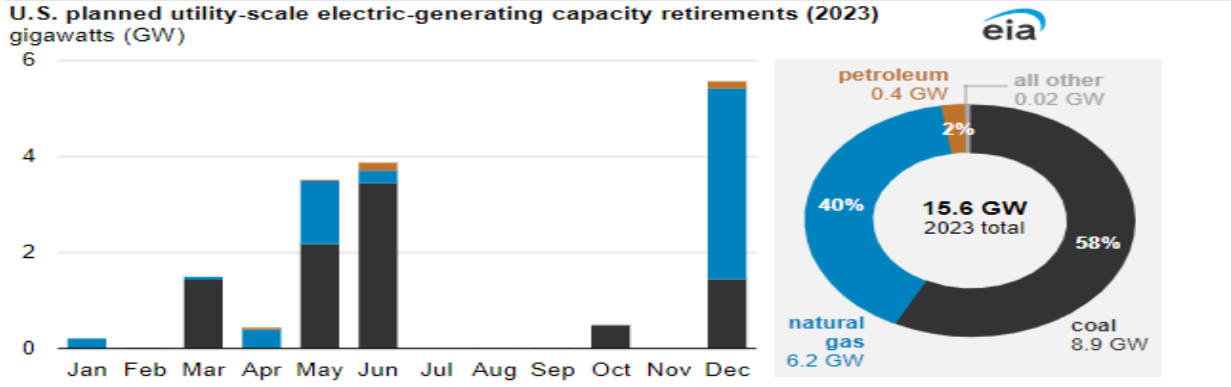

Fig. 1.1 Electricity Capacity additions and Retirements, 2023

EIA predicts that in 2023, a total of 15.6 GW of capacity will be in use. More than half of 2019's energy requirements would be met by wind energy capacity growth in Illinois, Texas, and Iowa. EIA data from January 10, 2023 shows that 65% of anticipated expansions would be fueled by wind energy. Among renewable energy sources, wind power typically uses more than 57% of the installed capacity. Furthermore, wind energy has a 6.6% market share globally. In addition to boosting its non-fossil fuel power output to 40% by 2030, India promised to create 60 GW of wind capacity by 2022. A rise in renewable energy sources is shown in Fig. 1.1 for the year 2023.

The past three publications of the Global Wind Energy Council (GWEC) paint a clear picture of the wind energy industry. According to the GWEC analysis, the global addition of wind-generated electricity in 2016 was far greater than 54 GW. The total electricity capacity rose by 12.6% to 486.8 GW. According to GWEC Secretary General Steve Sawyer, a zero-emission power system would be necessary by 2050 in order to combat climate change and meet development objectives. The paper claims that 4% of the electricity consumed in China, 20% in Spain and Cyprus, 20% in the United States, 5.5% in Canada, 6% in Germany, and 40% in Denmark is generated by wind energy.

The installed capacity will reach over 800 GW by the end of 2021, according to GWEC's five-year forecast, which anticipates over 60 GW of installations in 2017 and 75 GW of market growth per year through 2021. In terms of both annual additions and overall capacity, India had a boom in wind energy in 2013 and climbed to the fourth-largest market globally. By the end of June 2023, 3612 MW worth of new wind power generation capacity had been installed, according to the research. It was anticipated that 31,177 MW would be attained by the end of March 2017. The data for wind energy in 2023 are shown in Fig. 1.2.

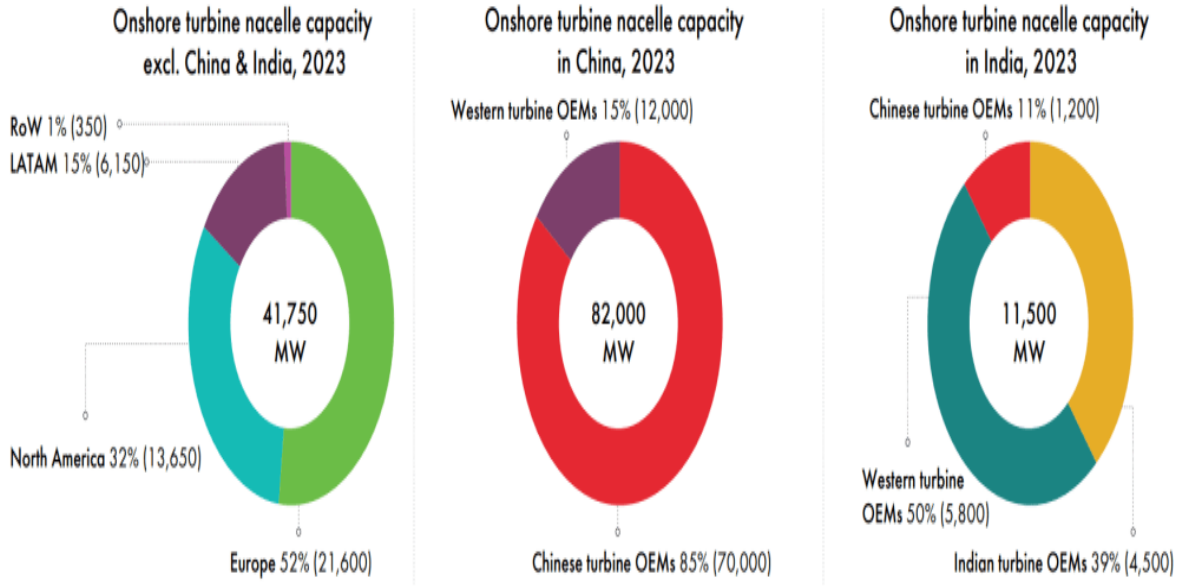

Fig. 1.2 Wind Energy Data of Year 2023

Wind power often uses more than 57% of the installed capacity. A 6.6% market share was also held by wind energy globally. India committed to constructing 60 GW of wind energy capacity by 2022 and raising its non-fossil fuel power output to 40% by 2030. Europe will roll out wind technology at a far higher rate in the following five to ten years, claims a 2022 report, according to GWEC Secretary General Steve Sawyer. There will be more than 1000MW of installed capacity in 18 countries in Europe, 5 in Asia Pacific (China, Japan, Australia, and South Korea), 3 in North America (the US, Mexico, and Canada), 1 in Africa (South Africa), and 3 in the Middle East and North Africa by the end of 2022. In China, the US, Germany, India, Spain, the UK, France, Brazil, and Canada, wind energy capacity exceeds 10,000 MW. A range of mechanical and electrical components are utilized in a wind energy conversion system to convert kinetic energy (moving wind) into electrical energy. Fig. 1.3 illustrates the concept of transforming wind energy into electrical energy.

Due to its inexpensive cost, ability to convert electricity at varied wind speeds, and reduced mechanical stress, DFIG is used as the major component in the paper. The commercialization of DFIG-based wind generation systems (WGS) has benefited from these practical, economical, and technical advantages. Power electronic converters installed on both the grid and rotor sides are necessary for the DFIG-based WGS to function properly. MMC is the most promising technology for wind energy systems because of its versatility and capacity to achieve high nominal volumes.

ISSN Number: 2454-2024(Online)
International Journal of Technical Research & Science

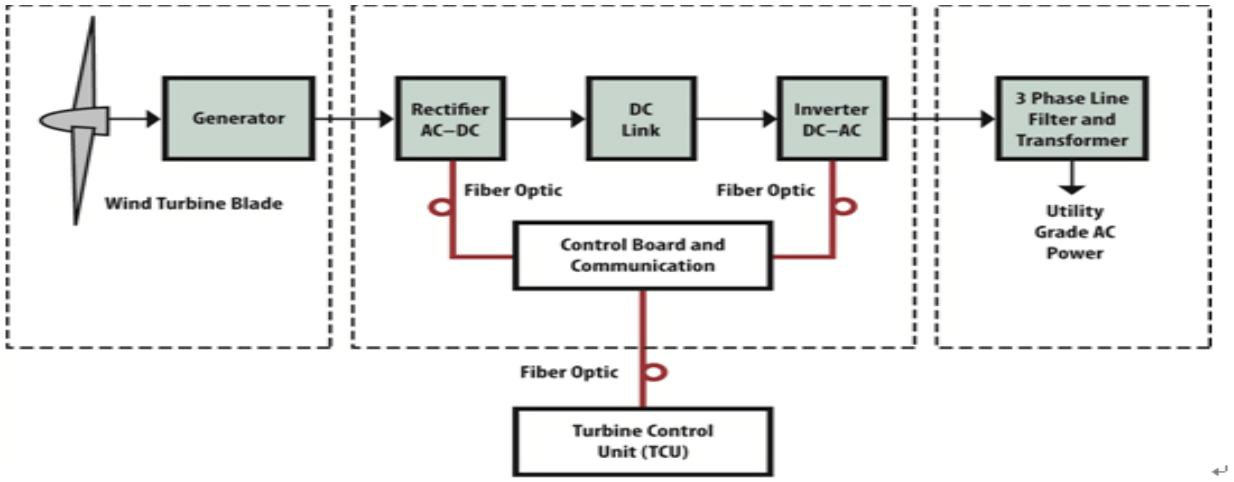

Fig. 1.3 Block Diagram of Wind Kinetic Energy to Electrical Energy Conversion System

Thus, in this paper, the benefits of both matrix converters (AC-AC conversion circuits with bi-directional conductive and bi-directional blocking switchers) and multilevel (high volume is obtained by low volume rating devices) will be utilized.

2. PROPOSED WIND ENERGY CONVERSION SYSTEM

As seen in Fig. 2.1, DFIG's stator is directly coupled to the grid by a coupling reactance. In contrast, the rotor is connected to the grid via a power electronic converter, or MMC, that is part of an electronic power-controlled system. The three DFIG features that can be changed are rotor current amplitude, rotor current frequency, and rotor current phase. The voltage and current at the point of common coupling (PCC) can be measured. The stator winding is directly connected to the 50 Hz grid, while the rotor is fed at a variable frequency through the MMC. The characteristics of the equivalent step-up transformer and the equivalent collector network can be used to calculate the output power of the equivalent DFIG, Vg, Ig, and Pg. The MMC converts the electrical power coming from the rotor side into a form that is consistent with the grid voltage of Vgscat and the constant frequency fg. The stator current can be regulated by adjusting the output current from the rotor PEC. The voltage loss across the stator resistance and leakage reactance is predicted to be minimal. The DFIG stator side voltage Vs and the frequency fs are matched to the grid voltage Vgsc and the grid frequency fg. On the rotor side of the PEC, however, the voltage and frequency are different from those on the grid side.

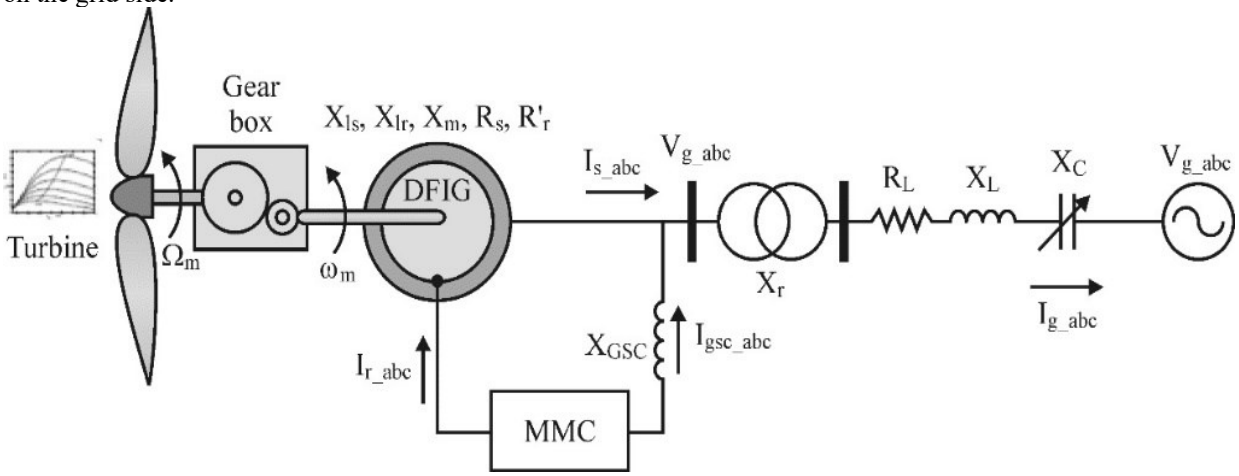

Fig. 2.1 Single Line Diagram of Proposed Multilevel Matrix Converter-Interfaced WECS Based on DFIG

The DC capacitor connecting the stator- and rotor-side converters allows power from the induction generator to be stored for later generation. The wound rotor is fed by the Power Electronics Converter VA slip rings while the stator is directly linked to the AC mains, allowing the DFIG to run at various rates in response to changing wind speed. A capacitor linked to the DC side serves as the source of DC voltage. A coupling inductor L is used to couple the grid side converter to the grid. The three-phase rotor winding is connected to the three-phase stator winding via slip rings

and brushes, and the stator winding is then directly connected to the grid. The workings of the DFIG are shown in Fig. 2.2.

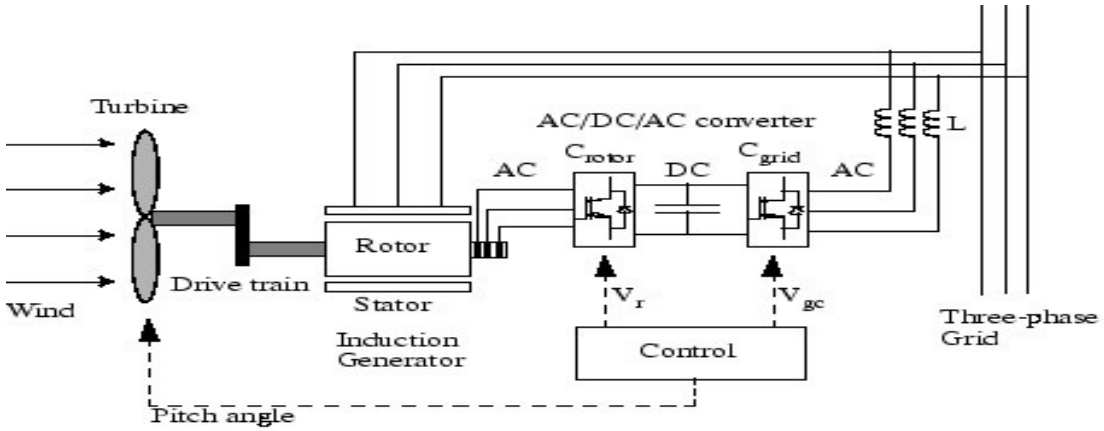

Fig. 2.2 Operating Principle of DFIG

3. MODELING OF WIND ENERGY CONVERSION SYSTEM

A turbine's hub and blades come together to form it. The wind turbine's inputs are wind speed, pitch angle, and rotor speed; its output is mechanical torque. The amount of wind energy that may be captured by WT is known as the aerodynamic power of the turbine (Pt). Model of a wind turbine like that in Fig. 3.1. The following can be used to write this power Pt:

$$P_t = \tau_t \omega_t \quad (1)$$

$$\frac{1}{2}\pi P R_{blade}^2 V_\omega^3 C_p(\lambda_{TSR}\cdot\beta) \quad (2)$$

Where

$\tau_t = turbineTorque$, $\omega_t = shaftspeed$, $V_w = windspeed$, $R_{blade} = radiusofblades$, $C_p = Efficiencycoefficient$, β= Pitch angle, $\lambda_{TSR} = Tipspeedratio$

$$\lambda_{TSR} = \frac{R_{blade}\,\omega_t}{V_\omega} \quad (3)$$

Efficiency coefficient is analyzed and approximated by a non-linear function: -

$$C_p(\lambda_{TSR}.\beta) = 0.2404\left(\frac{116}{\lambda t} - 0.4\beta - 5\right)e^{\frac{-12.5}{\lambda t}} \quad (4)$$

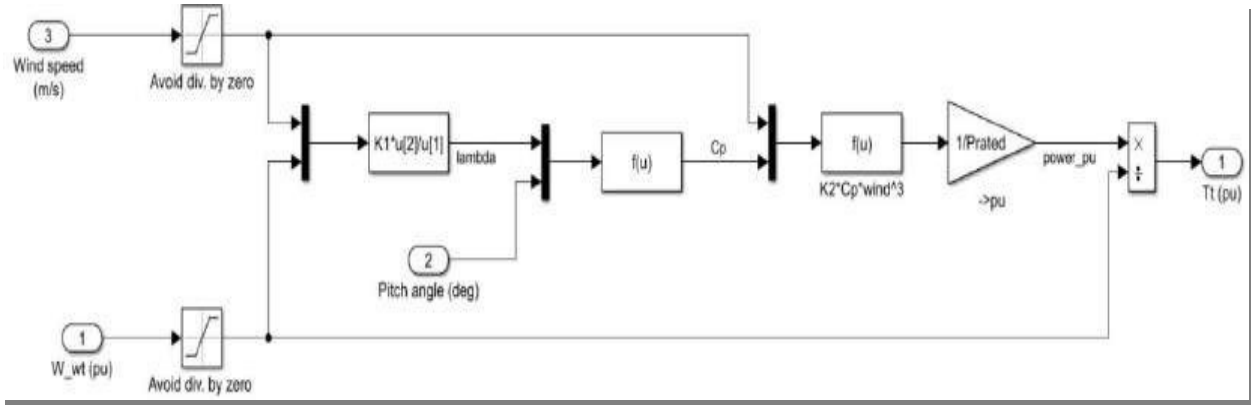

Fig. 3.1 Wind Turbine Model

The system's reaction is evaluated as soon as a flaw or disruption occurs. The drive train model is the most crucial one to have. Although this page explains two mass drive trains, many authors have only studied one mass drive train. Model of a wind turbine based on two mass systems is depicted in Fig. 3.2. An expression in the form of differential equations is as follows:

$$2Ht\frac{d\omega_t}{dt} = T_m - T_s \quad (5)$$

$$2Hg\frac{d\omega_t}{dt} = T_m - T_e \quad (6)$$

$$\frac{d\theta_{tw}}{dt} = (\omega_t - \omega_r r)\omega_B \quad (7)$$

$$T_s = K\theta_{tw} + D\left(\frac{dQ_{tw}}{dt}\right) \quad (8)$$

Ht=Turbine inertia, Hg= Generator inertia, wt= Turbine speed, wr= Rotor speed, Ts= Shaft torque, Tm= Motor torque, Te= electric torque, Qtw= shaft twist angle, K= Shaft stiffeners, D= damping coefficient.

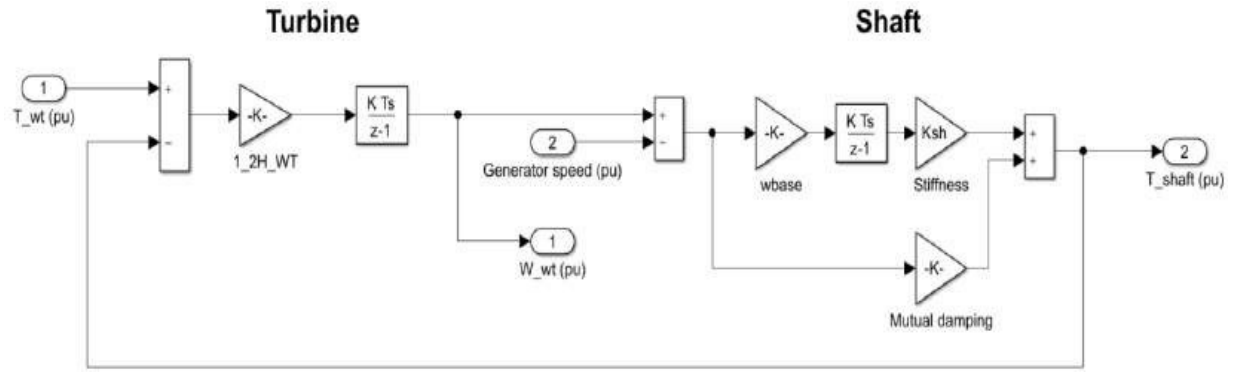

Fig. 3.2 Wind Turbine Drive Train Model Based on 2 Mass System

With the stator linked directly to the grid, it provides a controlled AC drive based on the WRIG idea. The rotor and grid are joined by a power electronic converter, also referred to as a back-to-back, matrix, multilayer, or MMC converter. A rotor side converter and a grid side converter are frequently both parts of this converter. Fig. 3.3 depicts a mathematical model power flow.

$$V_{dst} = R_s i_{dst} + \frac{d\varphi_{dst}}{dt} - \omega_s \Phi_{qst} \quad (9)$$

$$V_{qst} = R_s i_{qst} + \frac{d\varphi_{qst}}{dt} - \omega_s \Phi_{qst} \quad (10)$$

$$V_{dr} = R_r i_{dr} + \frac{d\varphi_{dr}}{dt} - (\omega_s - \omega_r)\Phi_{dr} \quad (11)$$

Active and reactive power at the stator as:

$$P_s = V_{dst} i_{dst} + V_{qst} i_{qst} \quad (12)$$

$$Q_s = V_{qst} i_{qst} + V_{dst} i_{qst} \quad (13)$$

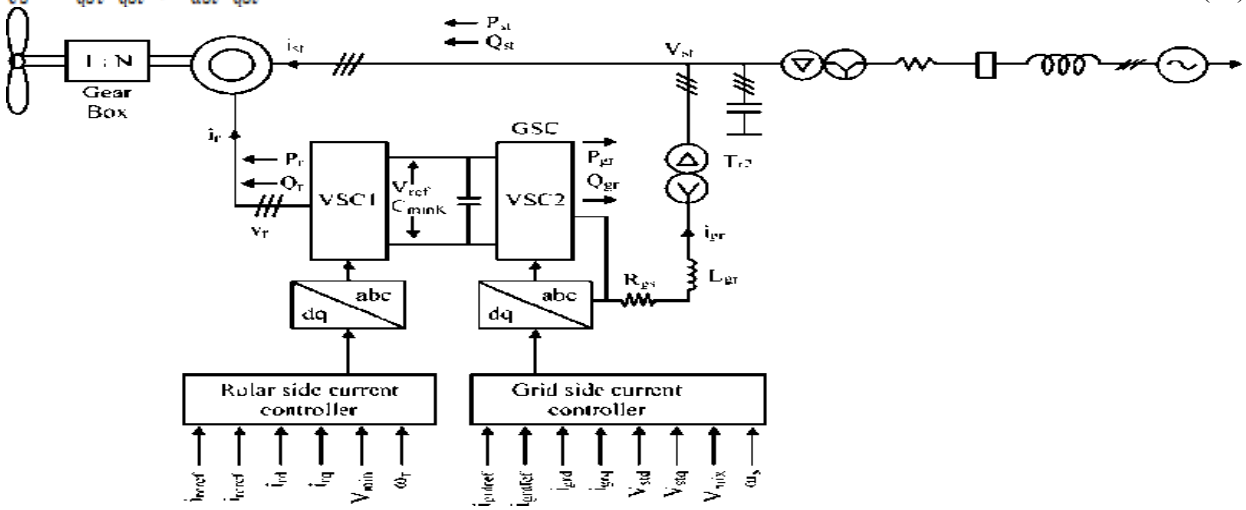

Fig. 3.3 Power Flow and Mathematical Model

$P_r = P_{gc} + P_{dc}$ (14)

$P_{rc} = V_{dr} i_{dr} + V_{qr} i_{qr}$ (15)

$P_{gc} = V_{dgc} I_{dgc} + V_{qgc} I_{qgc}$ (16)

$P_{dc} = V_{dc} I_{dc} = -C V_{dc} dV_{dc}/dt$ (17)

Where

P_r – Active power at RSC

P_{gc} – Active power at GSC

P_{dc} – Active power at DC

4. CONVERTER MODEL

Back-to-back In wind turbines, VSC is typically used to connect two pulse width modulation inverters, RSC and GSC, via a DC link. RSC injects an AC voltage into the rotor at the slip frequency, while GSC maintains a constant DC link voltage. This idea is essentially the power conversion model. The mathematical model of the converter has a power balance equation.

$P_r=P_{gc}+P_{dc}$ (18)

$P_{rc}=V_{dr}i_{dr}+V_{qr}i_{qr}$ (19)

$P_{gc}=V_{dgc}i_{dgc}+V_{qgc}i_{qgc}$ (20)

$P_{dc}=V_{dc}I_{dc} = -CV_{dc}\, dV_{dc}/dt$ (21)

Where

P_r – Active power at RSC

P_{gc}– Active power at GSC

P_{dc} – Active power at DC

5. MULTILEVEL MATRIX CONVERTER (MMC)

The idea of including additional source voltage levels forms the foundation of any multilevel converter. It generates output voltage that is of greater quality when compared to traditional converters. This layout also offers a variety of evolving models with a high-voltage output by using power switchers. The condensed architecture of the multilevel matrix converter is shown in Fig. 5.1.

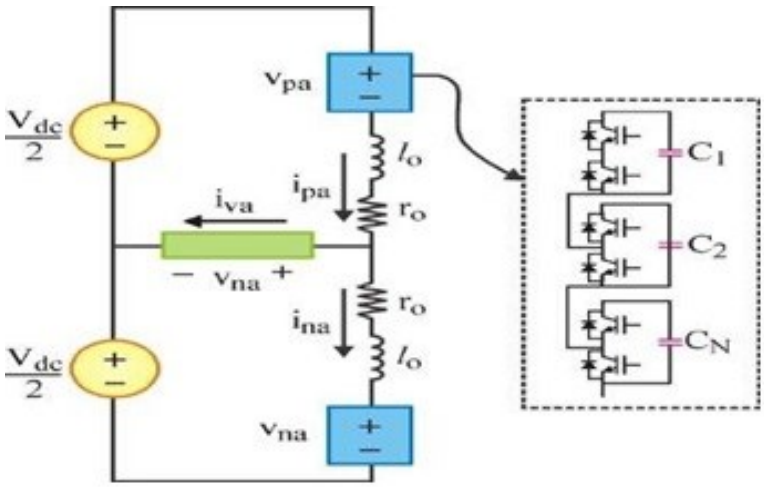

Fig. 5.1 A Single-Phase Multilevel Matrix Converter

Multilevel Matrix Converter has two separate operating modes. The terminal voltages are first created by the converter with two level switches on each side. Voltages across capacitors are controlled to be greater than the magnitudes of the lines bridging the two sides. Converters are switched at the three-voltage line-to-line voltage levels +Vcap, 0 and -Vcap.

An additional mode of operation has the converter generating voltage by switching levels at two on one side and three on the other. The line-to-line voltages of the converter are +2Vcap, +Vcap, 0, -Vcap, and -2Vcap at three switching levels. It comprises of a voltage source rectifier (VSR) made up of six switches and anti-parallel diodes. The six switches and extra series diodes that make up a current source inverter (CSI) are grouped together. As opposed to how it occurs in a typical matrix converter, power travels the other way from CSI to VSR terminals.

6. DEVELOPMENT OF CONTROL STRATEGY USING FUZZY LOGIC CONTROLLER

The active and reactive power management precision of the wind turbine driving the DFIG is the main objectives of the fuzzy controllers. Fuzzy logic controllers can be used to manage complex, unreliable, nonlinear, multivariable, time-varying, and adaptive systems like DFIG. The fuzzy logic controller's Sugeno and Mamdani approaches are the ones that are most frequently used. Using fuzzy logic control technologies, voltage deviation and waveform aberrations can be handled more effectively.

ISSN Number: 2454-2024(Online)
International Journal of Technical Research & Science

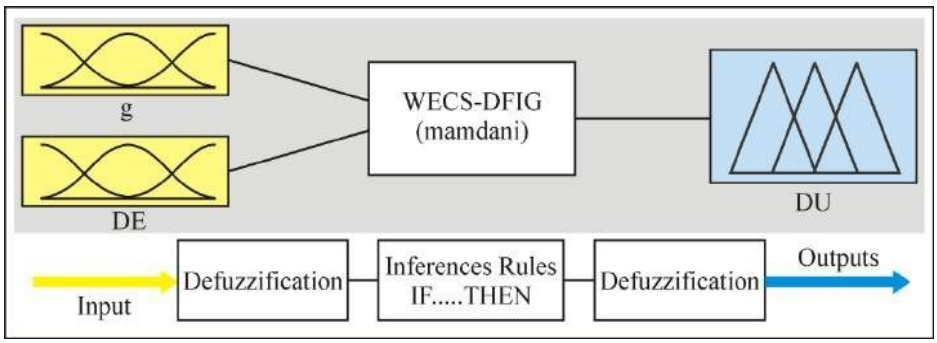

Fig. 6.1 Block Diagram of Fuzzy Control

6.1 Fuzzification

It is a method for decomposing system inputs and outputs using linguistic variables and membership functions. To translate linguistic rules into mathematical processes, fuzzy set degree of membership functions are calculated here. Any membership function can be adjusted little to reveal a large variation in the controller output. When reactive power control is required, the difference between the reference and measured levels of reactive power is maintained using three inputs.

6.2 Rule bases of the Fuzzy Logic Controller

The functioning of the fuzzy logic controller is carried out by different sets of rules that have been built after fuzzification and is based on the capability of the fuzzy logic controller to simulate multiple inferences concurrently. The fuzzy sets are defined as follows:
NB: Negative-Big; NM: Negative-Medium; NS: Negative-Small; AZ: About- Zero; PS: Positive-Small; NM: Positive-Medium; PB: Positive-Big.
Table 6.1 groups the fuzzy rules for the controller's output variable as a function of the input variables.

Table-6.1 Rule Matrix for Fuzzy Logic Controllers

	E							
				NS				
				NB				
				NB				
				NM				
				NS				
				AZ				
				PS				
				PM				

6.3 Membership Functions

For inputs, a triangle membership function is employed, and for the output, a Gaussian curve membership functions. The membership functions for the inputs and outputs as shown in Fig. 6.2.

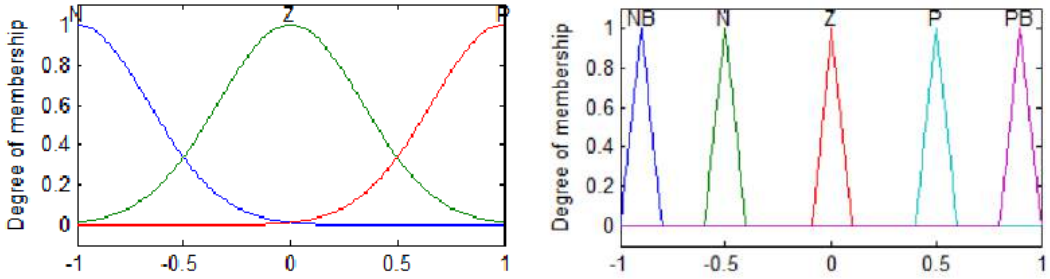

Fig. 6.2 The Membership Functions for the Inputs and Outputs

6.4 Defuzzification

As the name suggests, this method entails converting a fuzzily defined quantity into a definite quantity. The suggested control uses error changes (de(t)) and errors in the rotor current (e(t)) as inputs. The rotor voltage is the output. After examining the error signal pattern, its derivative, and the direct and quadratic rotor current components, the FLC

updates the output. There are scaling variables Ke and Kde. As shown in Fig.12, the output control signals are integrated to create the command signal after the du/dt has been multiplied by the output scale factor Kdu.

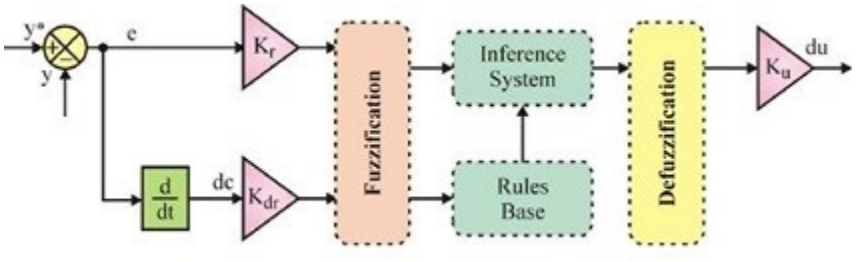

Fig. 6.3 Fuzzy Logic Structure

For the proposed FLC, d- and q-axis rotor current errors are the inputs to the direct and quadrate axis.
Developed Controller has following 7-segments membership functions

- Very Negative Big(VNB)
- Very Negative Medium(VNM)
- Very Negative Small(VNS)
- Zero(ZR)
- Very Positive Big(VPB)
- Very Positive Medium(VPM)
- Very Positive Small(VPS)

These make up the fuzzy rule set of the proposed controller, which produces the required outputs as a variety of membership functions and error membership functions. Table 6.2 details how to extract desired results utilizing the fuzzy rule set of the proposed developed fuzzy controller.

Table-6.2 Fuzzy Rules Set of Proposed Controller

Kp, Ki		**dE**						
		VNB	**VNM**	**VNS**	**VZR**	**VPB**	**VPM**	**VPS**
E	VNB	B	B	B	B	B	B	B
	VNM	S	B	B	B	B	B	S
	VNS	S	S	B	B	B	S	S
	ZR	S	S	S	B	S	S	S
	VPB	S	S	B	B	B	S	S
	VPM	S	B	B	B	B	B	S
	VPS	B	B	B	B	B	B	B

Fig. 6.3, 6.4, and 6.5 depict the error membership function, change in error of membership function, and duty cycle membership function of inputs and outputs developed for the proposed FL controller, respectively.

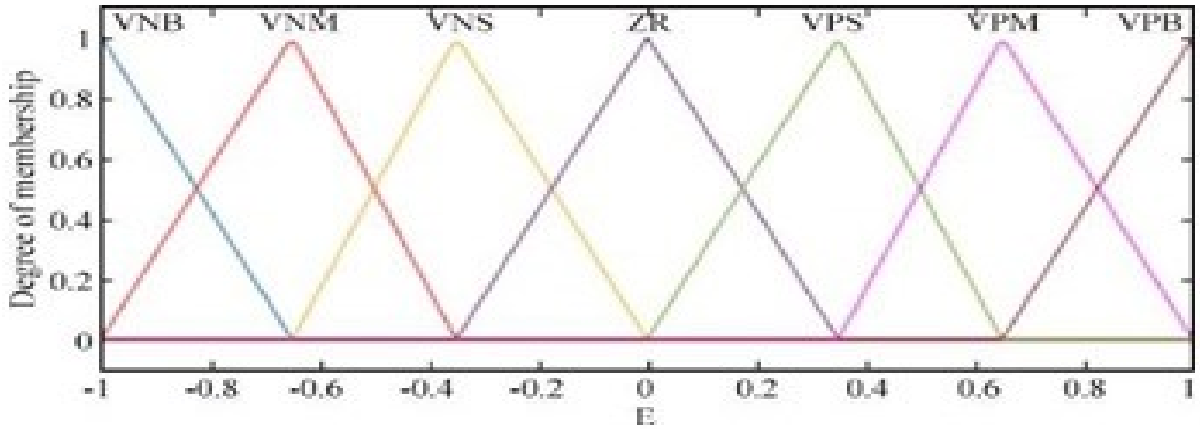

Fig. 6.3 Fuzzy Logic Controller with Error Membership Functions

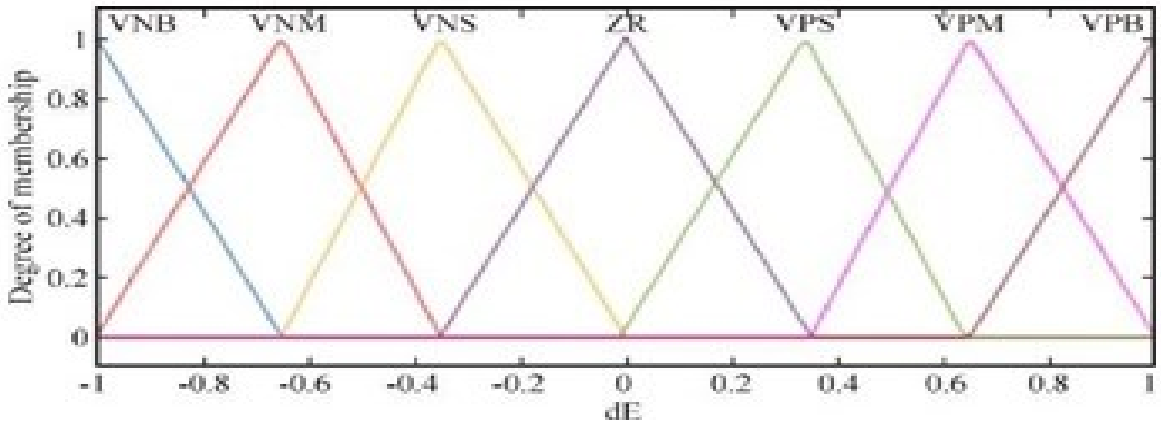

Fig. 6.4 Fuzzy Logic Controller with duty Cycle MF

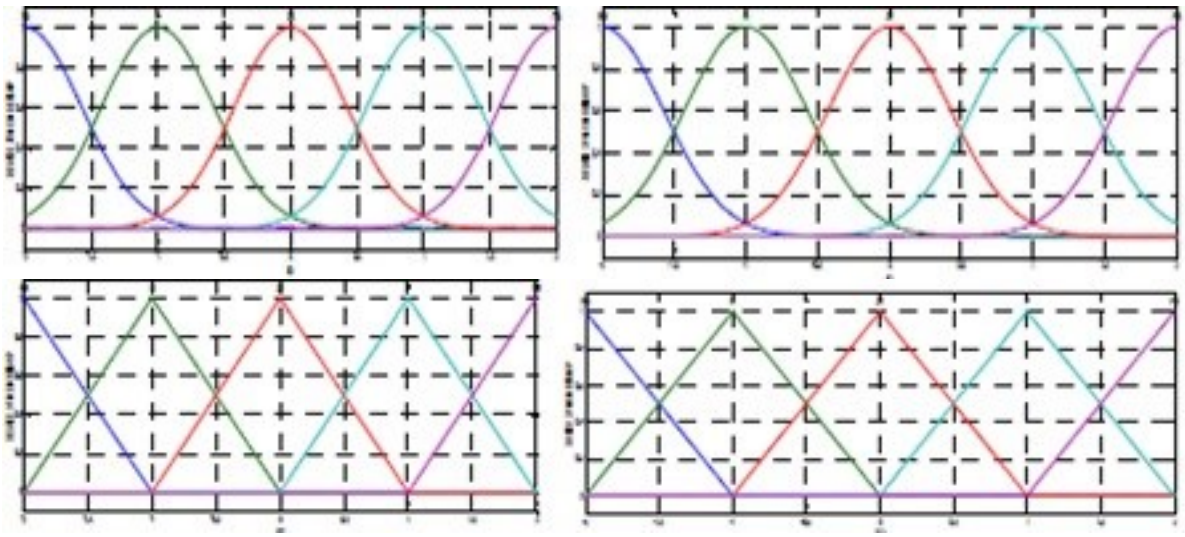

Fig. 6.5 Input and Output Membership Functions of Voltage Controller (for RSC and GSC)

7. MATLAB/SIMULINK

The multilevel Matrix converter and grid are modelled as a single unit of load resistance. Fig. 7.1 depicts the Simulink model of a wind turbine system, and Fig. 7.2 depicts the entire DFIG Simulink model-based wind generation system.

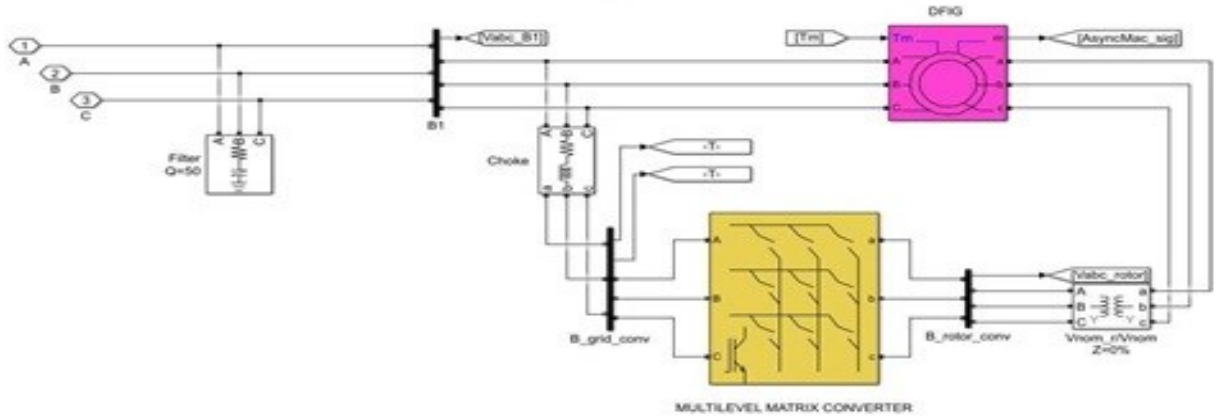

Fig. 7.1 Developed System for DFIG based WECS Interfaced Multilevel Matrix Converter

The Active and Reactive power regulation modes can be selected from a variety of functional building components in this intricate block diagram for parameters. Additionally, we have the flexibility and viability to simulate different error scenarios by setting the external reactive current (Iqref) on the grid side to zero.

ISSN Number: 2454-2024(Online)
International Journal of Technical Research & Science

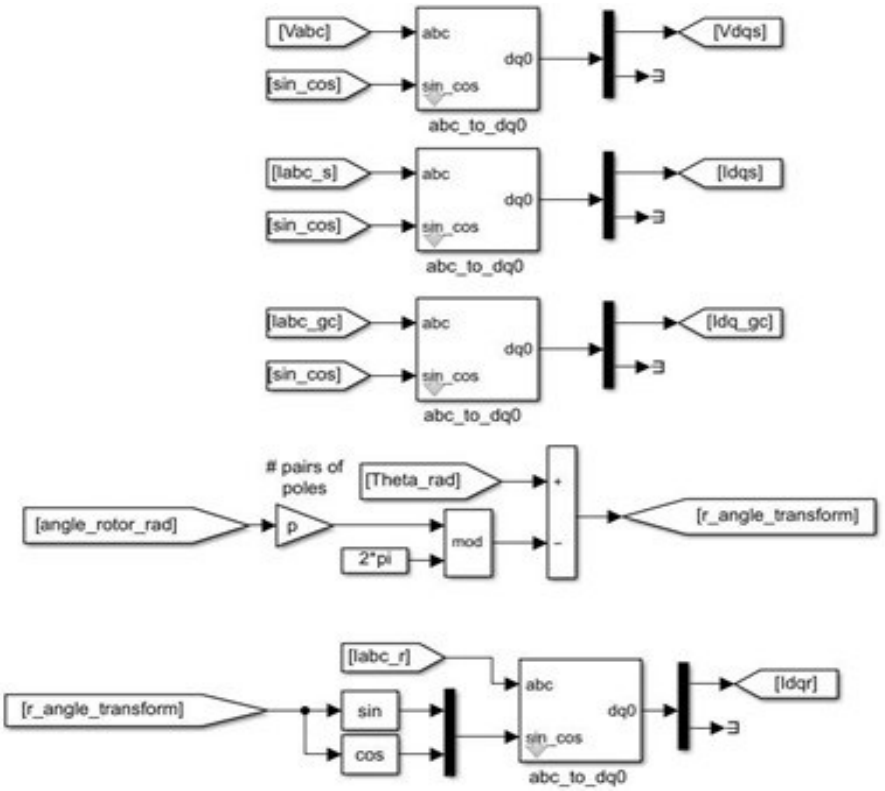

Fig. 7.2 ABC to DG Transformation Block

The multilevel matrix converter developed system with the DFIG configuration is used to experimentally prove and verify the proposed produced control technique. The MMC's input current is controlled by two controllers, which also independently control the active and reactive power exchanged with the grid. Two controllers are used to regulate the connected load or machine's current (magnetization and torque). Basic MMC Converter Modeling Block as shown in Fig. 7.3.

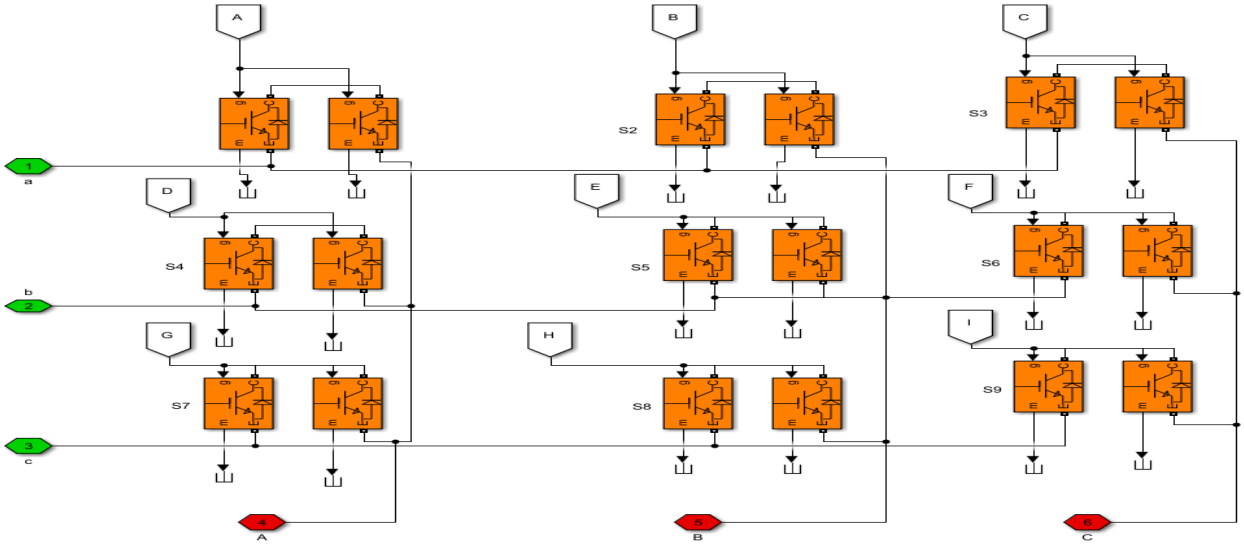

Fig. 7.3 Basic MMC Converter Modeling Block

The converter was coupled to a three-phase resistive load and a three-phase variance in the experimental setup, which can produce three-phase voltages between 0 and 420 V at 60 Hz. The output-side reference space vector can be controlled at will thanks to programmable output frequency and magnitude. MATLAB/Simulink is used to develop the MMC model. Ten DFIG are required to equal the wind farm. The cables are 30 km long and include five replicas. Fuzzy Logic Inputs to DFIG Wind Turbine as shown in Fig. 7.4.

ISSN Number: 2454-2024(Online)
International Journal of Technical Research & Science

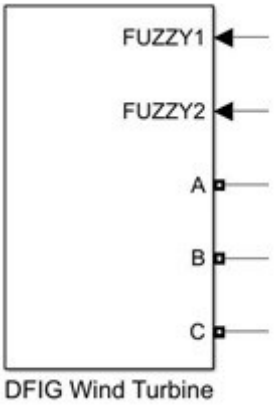

Fig. 7.4 Fuzzy Logic Inputs to DFIG Wind Turbine

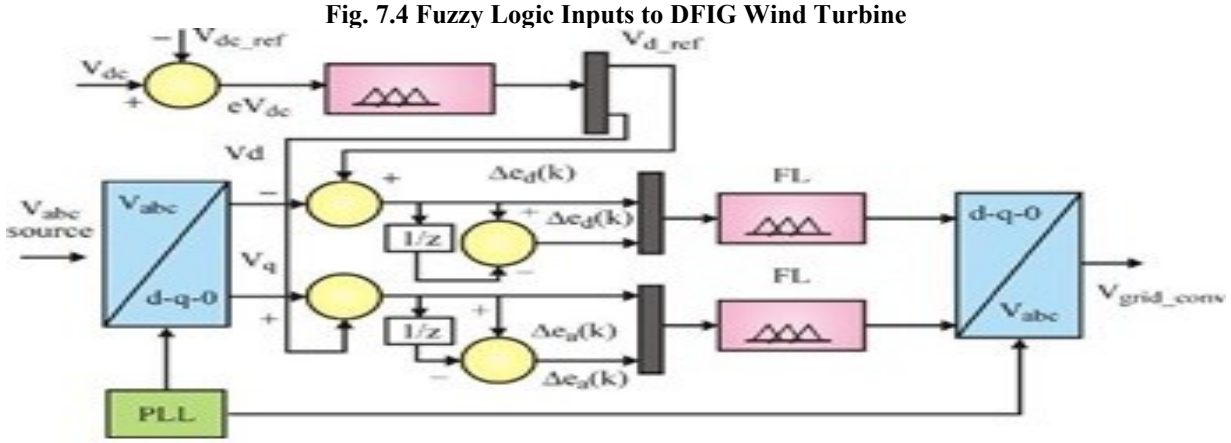

Fig. 7.5 Control Circuit with Fuzzy Logic Controller

Table-7.1 Rule Base Table of Proposed Fuzzy Controller

		e(t)		
		P	**EZ**	**N**
de(t)	**P**	**PB**	**N**	**NB**
	EZ	**PB**	**EZ**	**NB**
	N	**PB**	**P**	**NB**

Fuzzification, fuzzy rules, and defuzzification are built in the MATLAB software's FIS editor. The created rules are then applied using the fuzzy controller, which is integrated into a simulation file. The figure depicts the suggested fuzzy controller for managing DFIG's reactive power. Proposed fuzzy controller to control reactive power of DFIG as shown in Fig. 7.6.

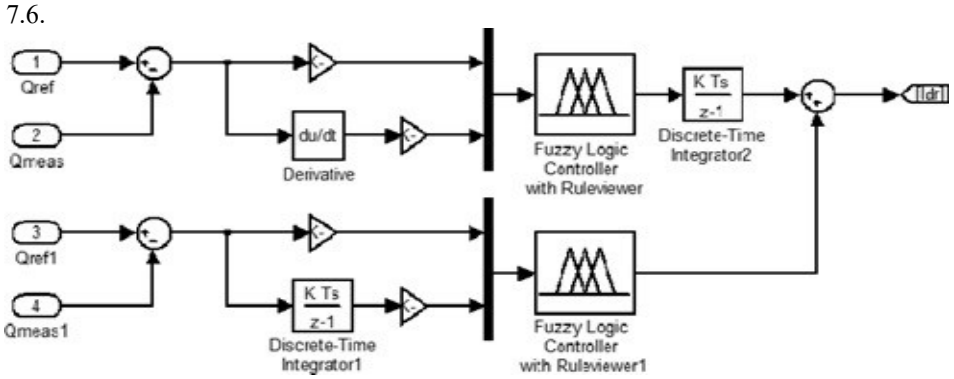

Fig. 7.6 Proposed Fuzzy Controller to Control Reactive Power of DFIG

This fuzzy logic controller, which has two inputs and one output, is shown in Fig. 7.7 The error signal is determined by comparing the actual and reference d- component voltages. The error signal e (k) and change in error ed (k) are inputs to the fuzzy logic controller's q- components. Fuzzy Set Rule Viewer of Outputs as shown in Fig. 7.8

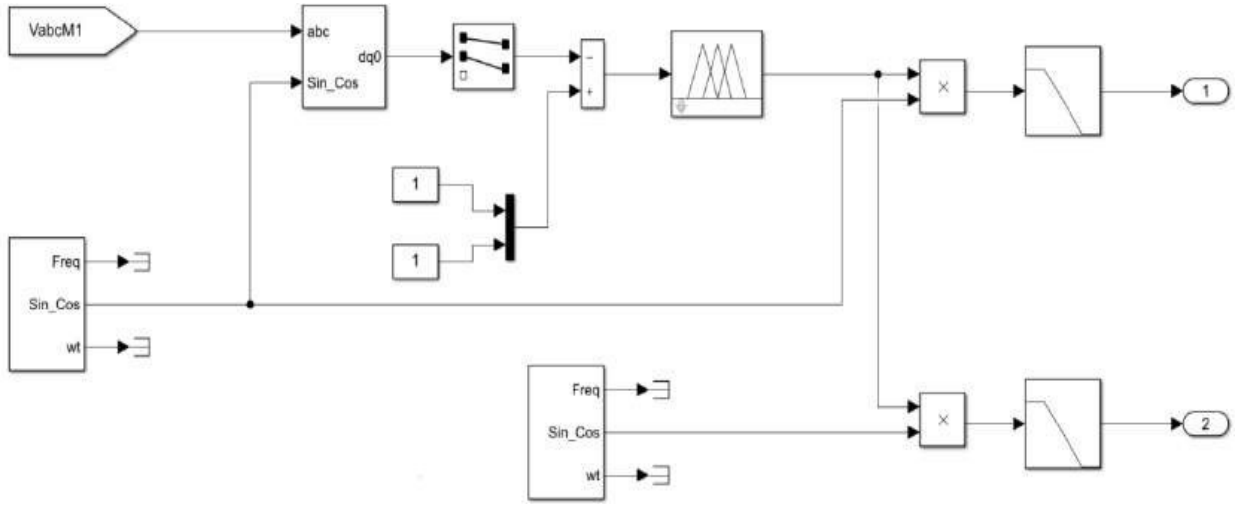

Fig. 7.7 Simulink Model of Fuzzy Controller

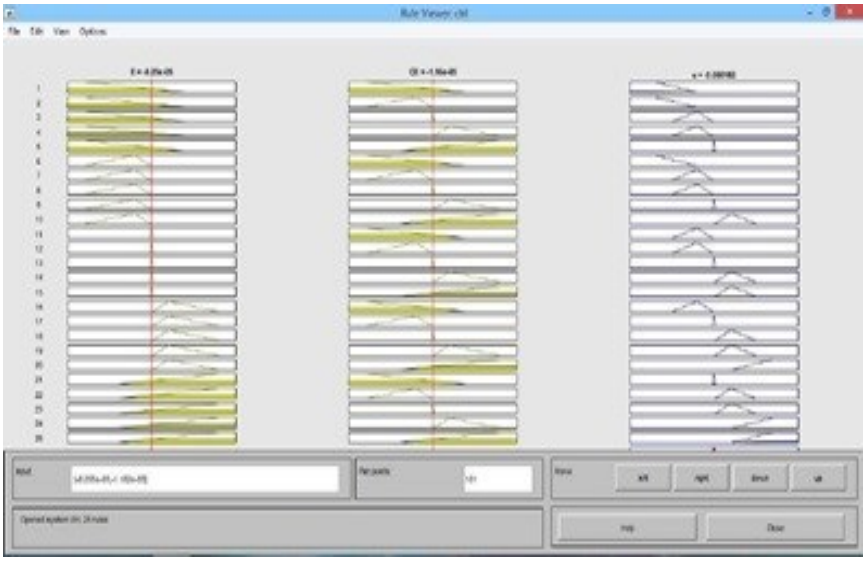

Fig. 7.8 Fuzzy Set Rule Viewer of Outputs

8. RESULTS AND DISCUSSIONS

This chapter uses MATLAB/Simulink to simulate the proposed fuzzy logic controlled multilevel matrix converter interfaced Doubly Fed Induction Generator based wind energy conversion system under a variety of balanced and unbalanced conditions. These conditions include changing load, changing wind speed, changing grid voltage sag and swell, changing three-phase and single-phase fault conditions, and changing load sag and swell. The simulation and experiment should be divided into two phases: In the first stage, simulations are performed on a typical converter. In the second stage, a 3 -3 multilevel matrix converter is built in order to assess the multilevel matrix converter's operating principles. The simulation outcomes of the created fuzzy control system will be contrasted with those of conventional control.

8.1 Simulation Results of various parameters during Constant rated Wind Speed (12m/s) and Resistive Load (3KW)

For the first time, simulation data displays a constant wind speed of 12 m/s in this situation. A resistive load is applied in this simulation scenario. Constant wind speed is usually a case to analyse in order to see more simulation results in later cases because wind speeds constantly fluctuate at different penetration levels. The MATLAB simulation results for the created DFIG-based WECS are shown in Fig. 8.1.

Fig. 8.2 shows the simulated results for constant wind speed (s), generator speed (m), generator output power (Pac), and DFIG phase to phase voltages (Vab,,Vbc, and Vac).1. A voltage and current of 230V and 10.1A are produced. At constant wind speeds of 12 m/s, the electromagnetic and mechanical torque, DFIG voltage and current, rms output voltage, and rms output current of the generator were all simulated. Generator voltages Vd and Vq are 70V and 140V, respectively, while generator rms voltage and current remain constant at 180V and 8A. The Id and Iq generator currents are 4A and 9A, respectively.

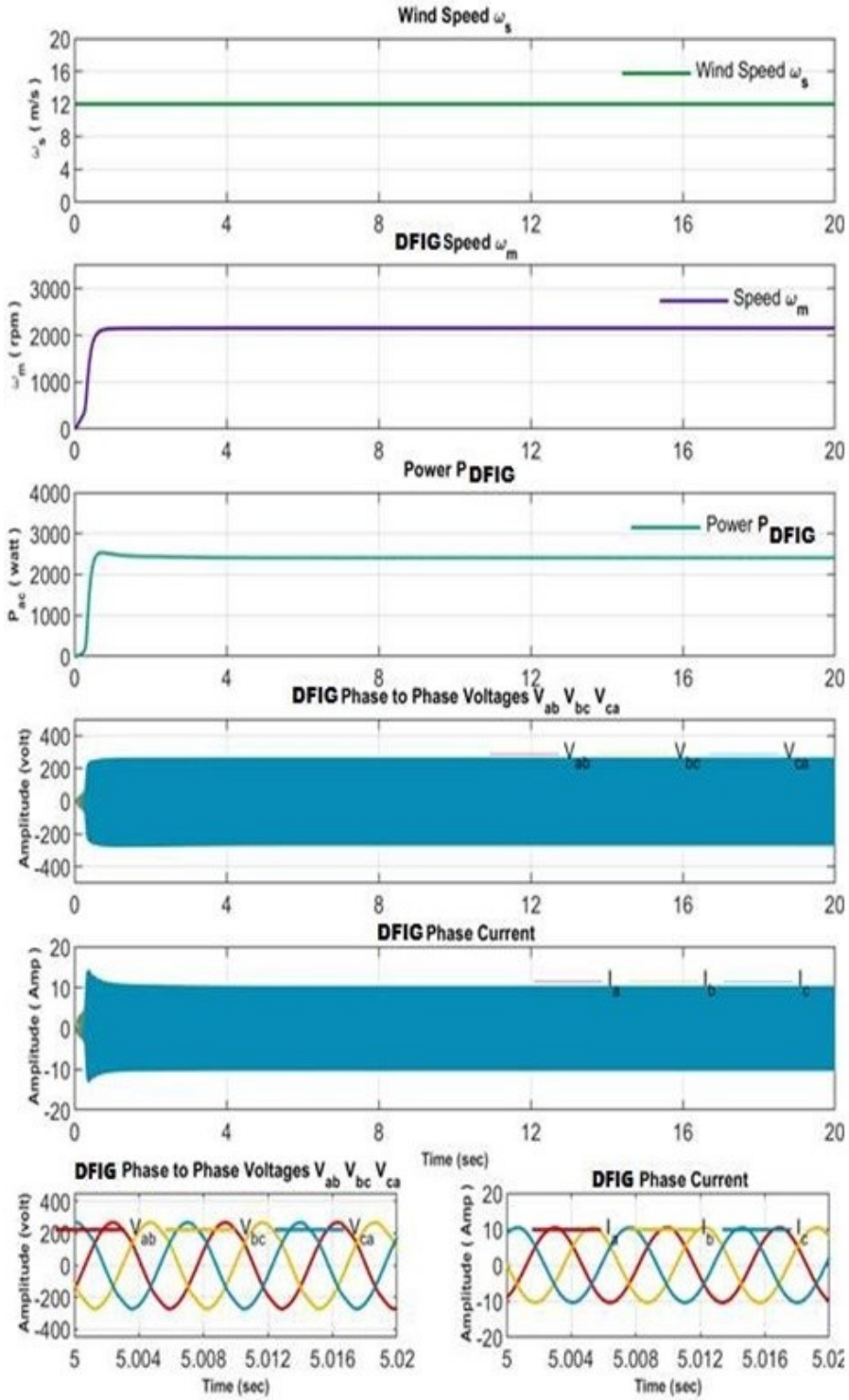

Fig. 8.1 Simulation Results for DFIG based WECS at Constant Wind speed of 12m/s, Waveform of Wind speed Ws, DFIG speed Wm, DFIG Output Power P_{DFIG}, DFIG Phase to Phase Voltages $VabVbcVca$, DFIG Phase Current

ISSN Number: 2454-2024(Online)
International Journal of Technical Research & Science

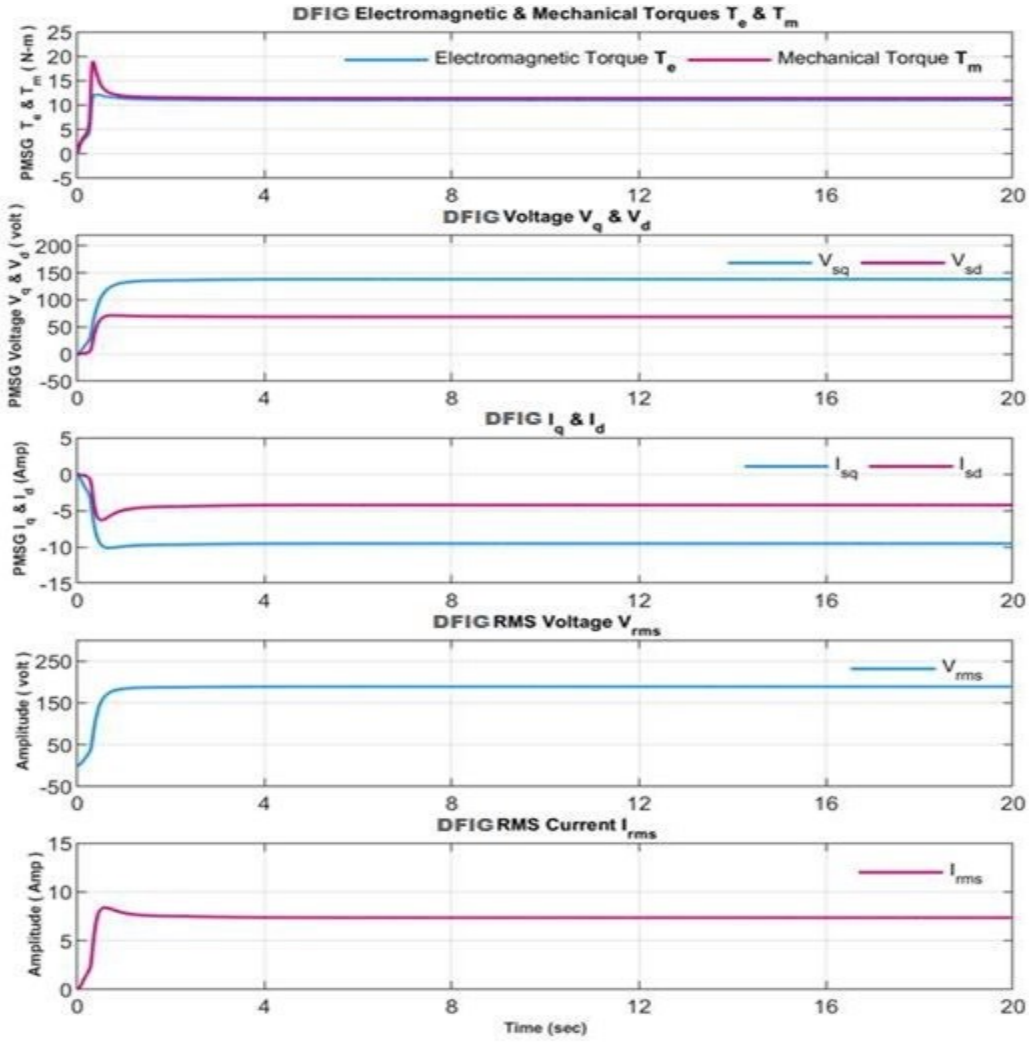

Fig. 8.2 Simulation results for DFIG based WECS for Constant Wind Speed of 12m/s, Waveform of Electromagnetic and Mechanical torque, DFIG Voltage, DFIG Current, DFIGrms Output Voltage and DFIG RMS Output Current

Fig. 8.3 displays the MMC's various waveforms, including (a) the duty ratio, (b) the output voltage, and (c) the output current. The values for the various parameters are MMC output voltage of 500V and MMC output current of 40A, as can be seen in Fig. 8.3.

The grid output voltage and current waveforms, which are shown in Fig. 8.4, is the subject of another analysis.

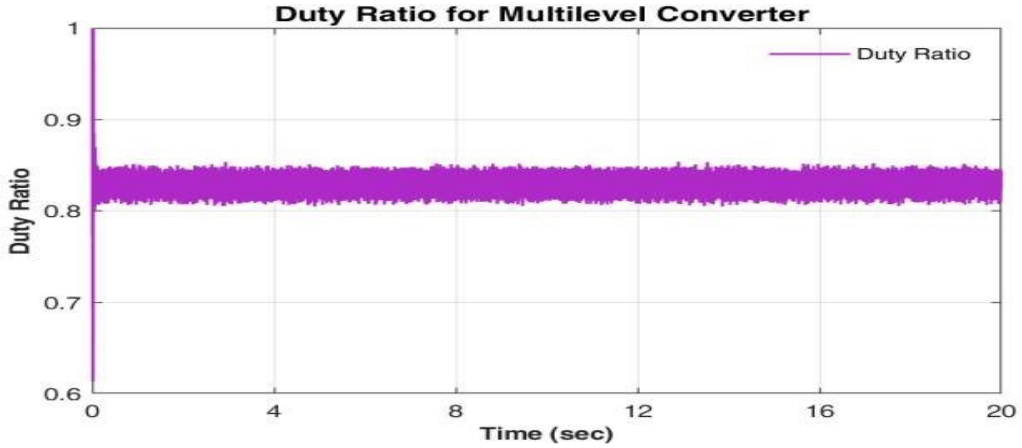

Fig. 8.3 Simulation Waveform of MMC Duty Ratio

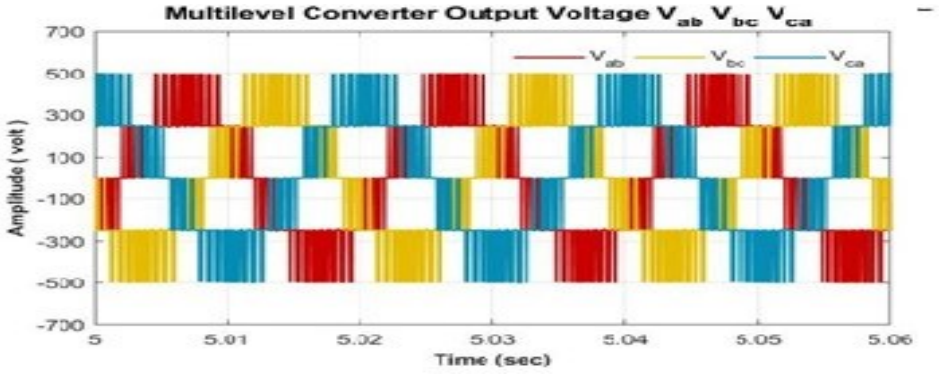

Fig. 8.4 Simulation Waveform of MMC Output Current

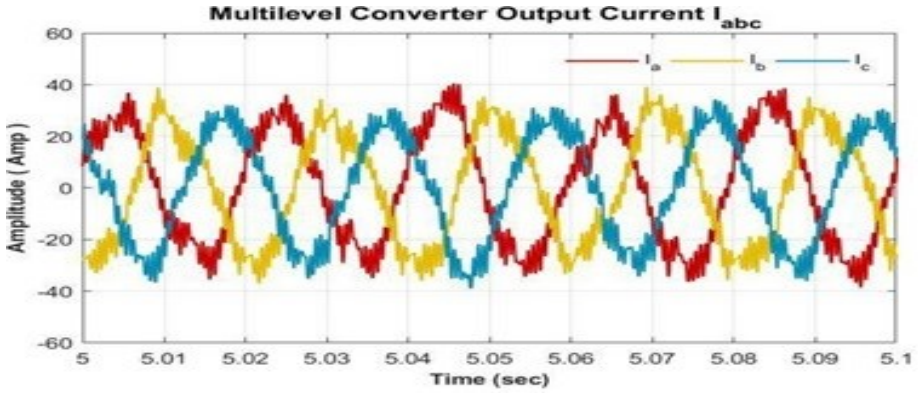

Fig. 8.5 Simulation Results for DFIG based WECS for Constant Wind Speed of 12m/s, Waveform of MMC

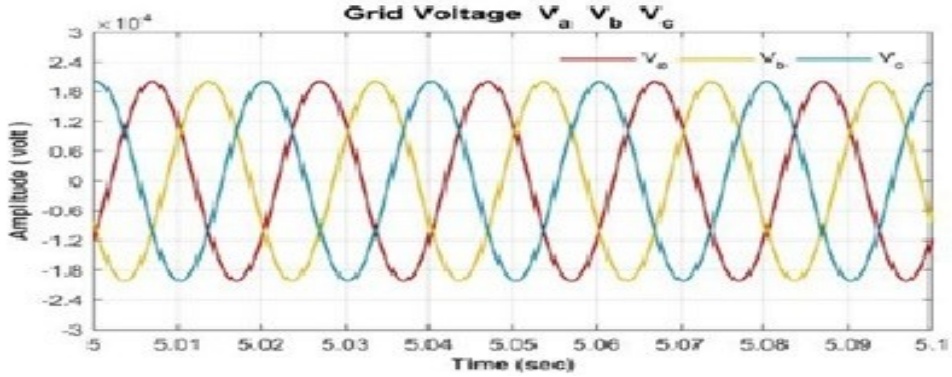

(a)

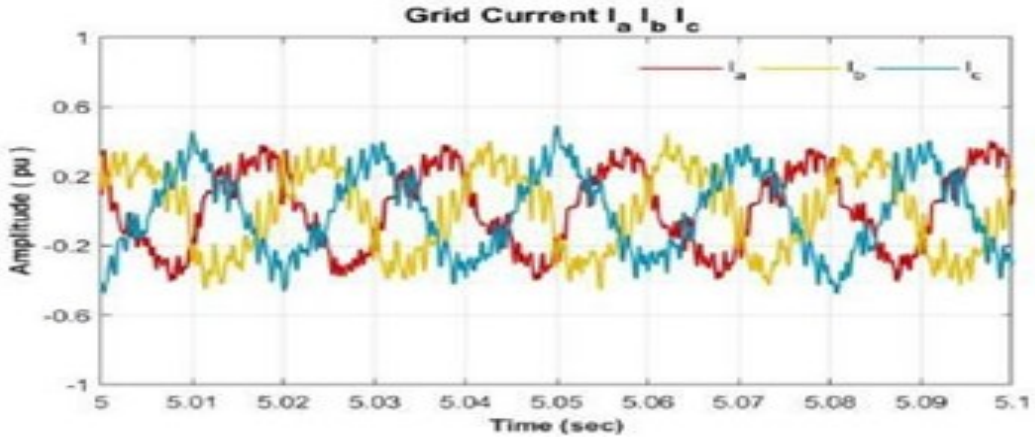

(b)

Fig. 8.6 Simulation Results for DFIG based WECS for Constant Wind Speed of 12m/s, (a) Waveform of Grid Output Voltage and (b) Waveform of Grid Output Current

8.2 Simulation Results of Different Parameters during Impulse variation in Wind speed

In the second scenario, the wind speed is changed as an impulse function from 12 m/s to 8 m/s and back from 8 m/s to 12 m/s while the load is kept constant at 3 KW.

Fig. 8.7, sourced. As the time passes from 0 to 7 seconds, or from t=0 sec to t=7 sec, the wind speed that is being observed is 12 m/s. The wind speed steps from 12 m/s to 8 m/s at time t=7 sec, and then steps back from 8 m/s to 12 m/s at time t=14 sec. When the time changes from 7 seconds to 14 seconds, the generator's output switches from 2.4KW to 1.1KW. The generator's output stays constant at 2.4 KW after 14 seconds.

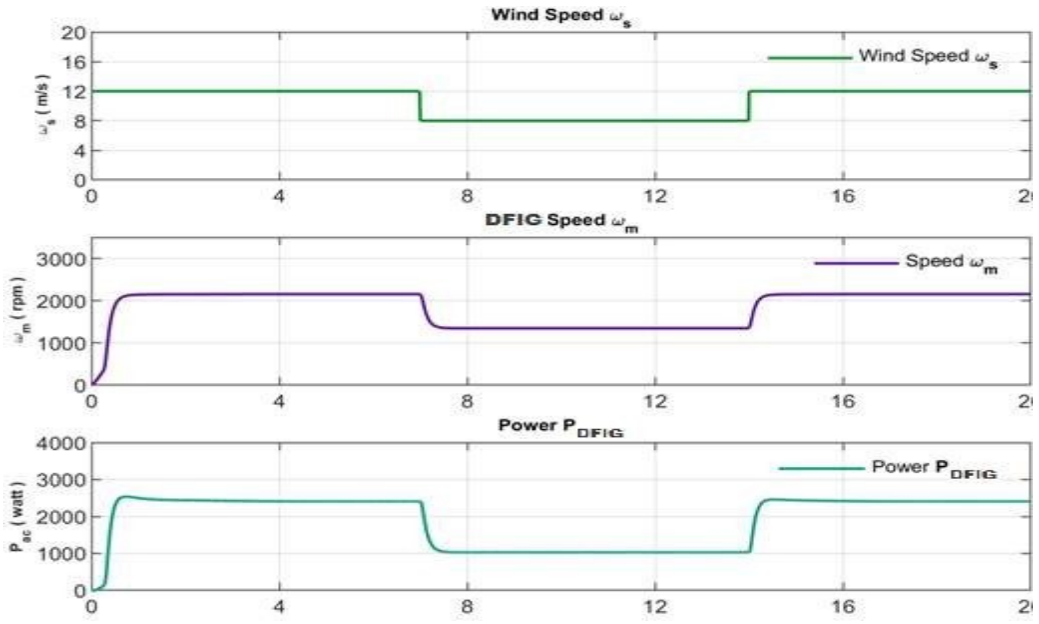

(a)

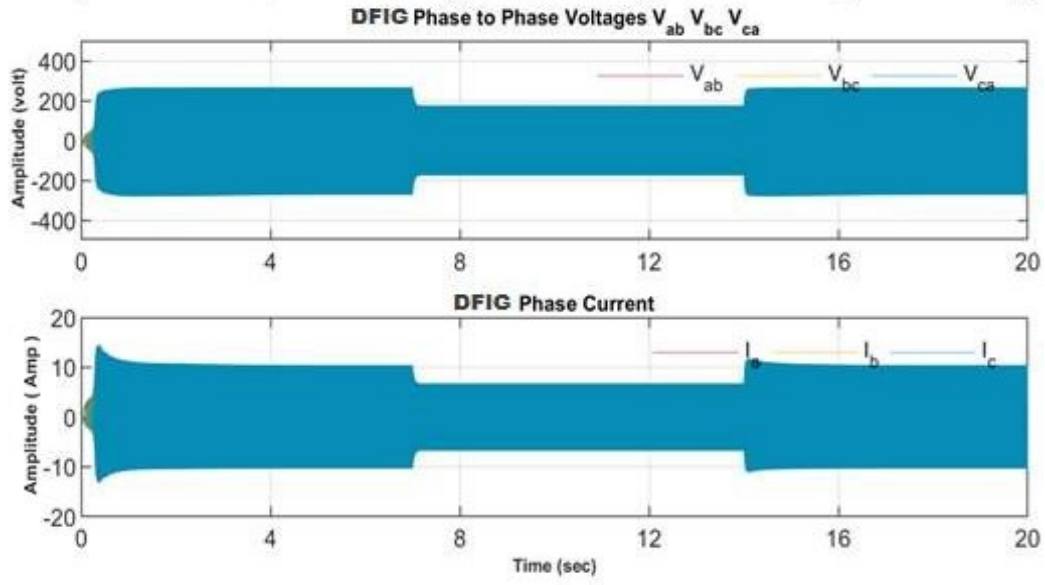

(b)

Fig. 8.7 (a) Simulation Waveform of Wind Speed, DFIG speed, DFIG Output Power, (b) DFIG Phase to Phase Voltages, DFIG Phase Current at during Impulse Variation in Wind Speed from 12 m/s to8 m/s to 12 m/s with Constant Load

The DFIG phase current and DFIG phase to phase voltage are depicted and explained in Fig. 8.8. The output voltage declines from 280 to 180 V for a duration of 7 to 14 seconds under steady-state circumstances. Both the output voltage and current have sinusoidal forms. Similar to this, output current decreases from 14.5 A to 6 A after t=14 seconds. The simulation results are shown in Fig. 8.9 for the mechanical and electro-magnetic torque generators' RMS output voltage, current, and voltage.

ISSN Number: 2454-2024(Online)
International Journal of Technical Research & Science

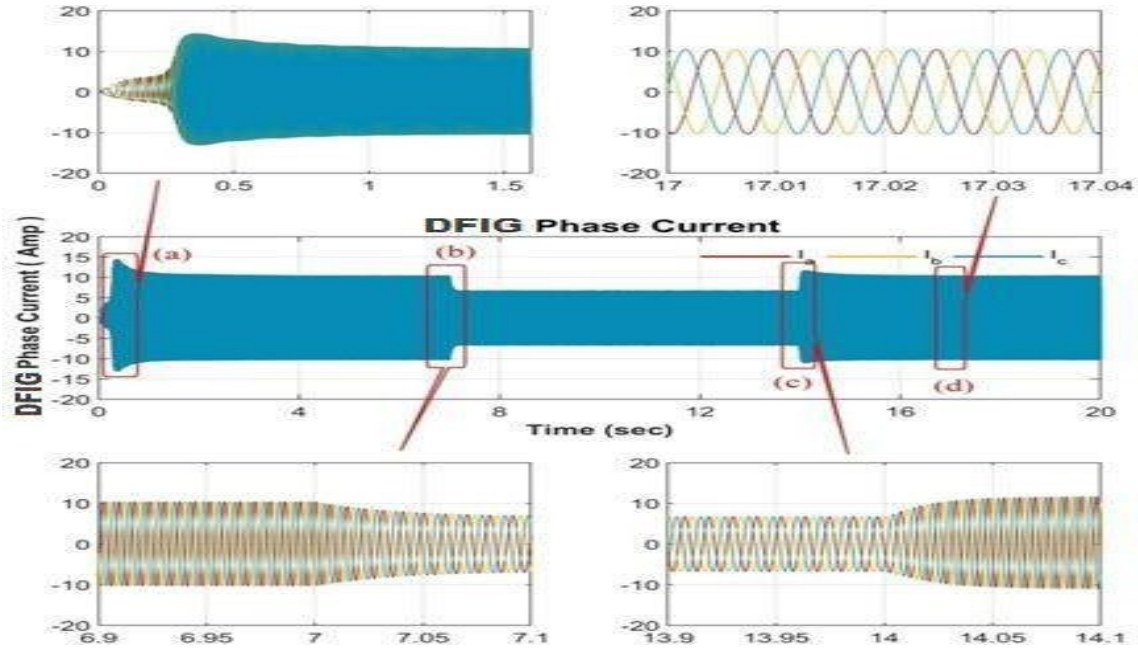

Fig. 8.8 Simulation Waveform of DFIG Phase Current and DFIG Phase to Phase Voltage at During Impulse Variation in Wind Speed from 12 m/s to 8 m/s to 12 m/s with Constant Load

As depicted in Fig. 30, the values of the various generator parameters change over a period of 7 to 14 seconds, causing the generator's RMS voltage to decrease from 180V to 130V over a predetermined amount of time. The generator's current decreases in a similar manner, going from 7.5 A to 5A. Maximum output values frequently stabilise at t=14 seconds. The electromagnetic and mechanical torque also varies from 11 N-m to 8 N-m during the wind speed impulse variation between 7 and 14 sec. In addition, mechanical torque rises in the obverse direction between 5 N-m and 10 N-m.

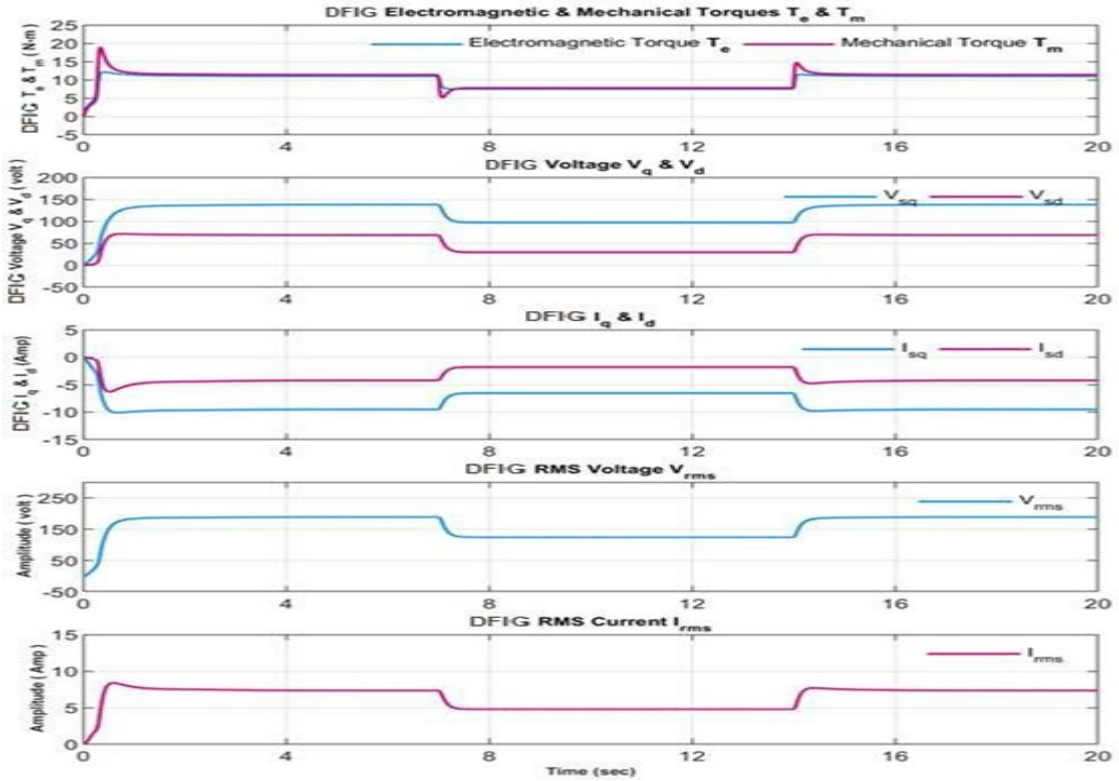

Fig. 8.9 Simulation Waveform of Electromagnetic and Mechanical torque, DFIG voltage, DFIG current, DFIG RMS Output Voltage and DFIG RMS Output Current at During Impulse Variation in Wind Speed from 12 m/s to 8 m/s to 12 m/s with Constant Load

ISSN Number: 2454-2024(Online)
International Journal of Technical Research & Science

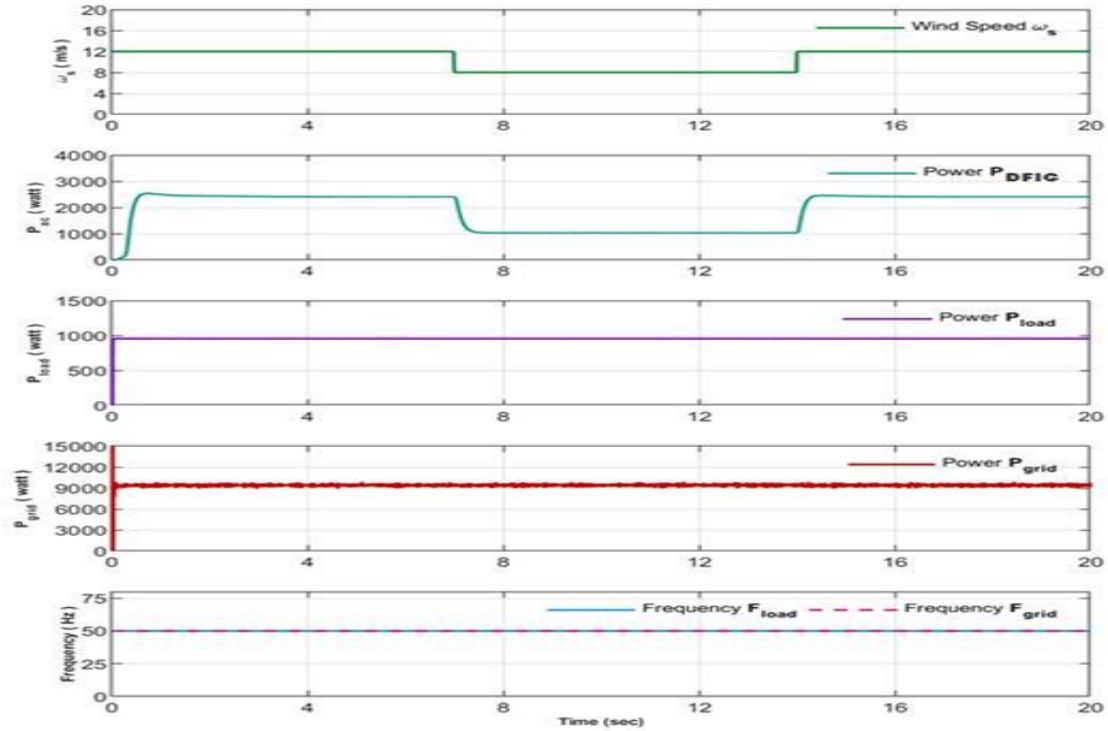

Fig. 8.10 Simulation Waveform of Wind Speed, DFIG Output Power, Load Output Power, Grid Power, Load Frequency and Grid Frequency during Impulse Variation in Wind Speed from 12 m/s to 8 m/s to 12 m/s with Constant Load

According to Fig. 8.11, the generator's output power decreases from 2.4 KW to 1.1 KW during the times t=7 and t=14. The grid, load, and load power waveforms are all displayed, and the grid, load, generator, and increasing wind speed waveforms are all constant at 50 Hz.

The grid power and load power stay fixed at 9000W and 900W, respectively, from time t=0 sec to t=14 sec.

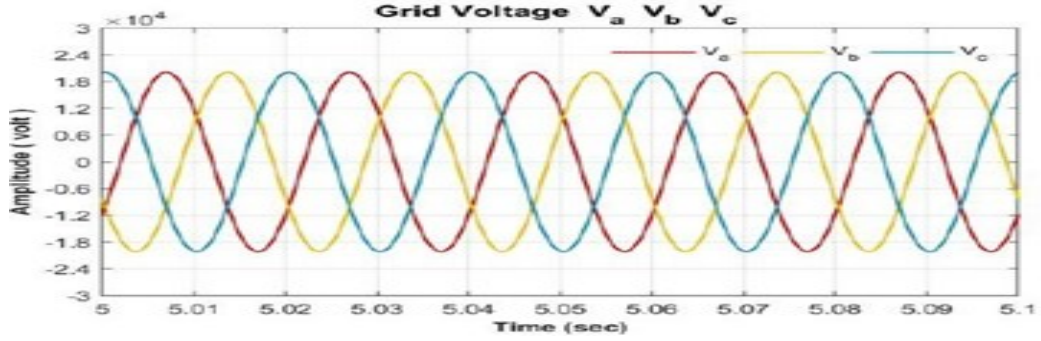

(a)

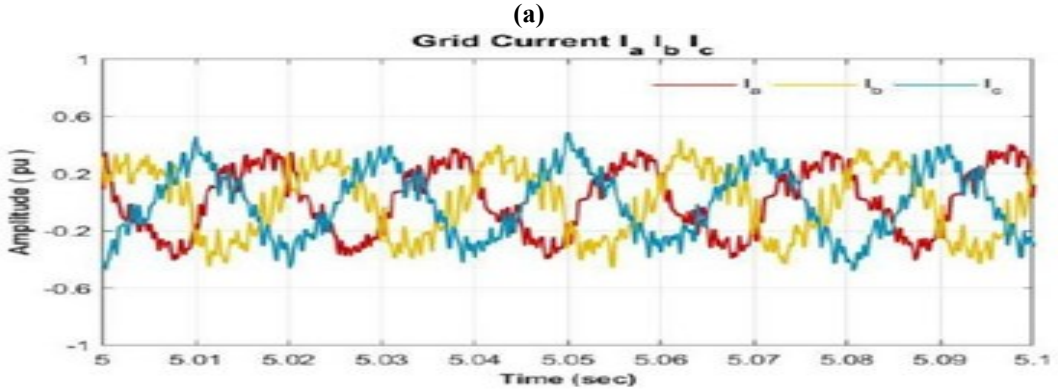

(b)

Fig. 8.11 Simulation (a) Waveform of Grid Output Voltage (b)Waveform of Grid Output Current During Impulse Variation in Wind Speed from 12 m/s to 8 m/s to 12 m/s with Constant Load

Fig. 8.12 depicts the simulated waveforms for the transient behavior of converters-based WECS with DFIG, active and reactive power, rotor speed, and torque to demonstrate that the MMC-based control technique performs better.

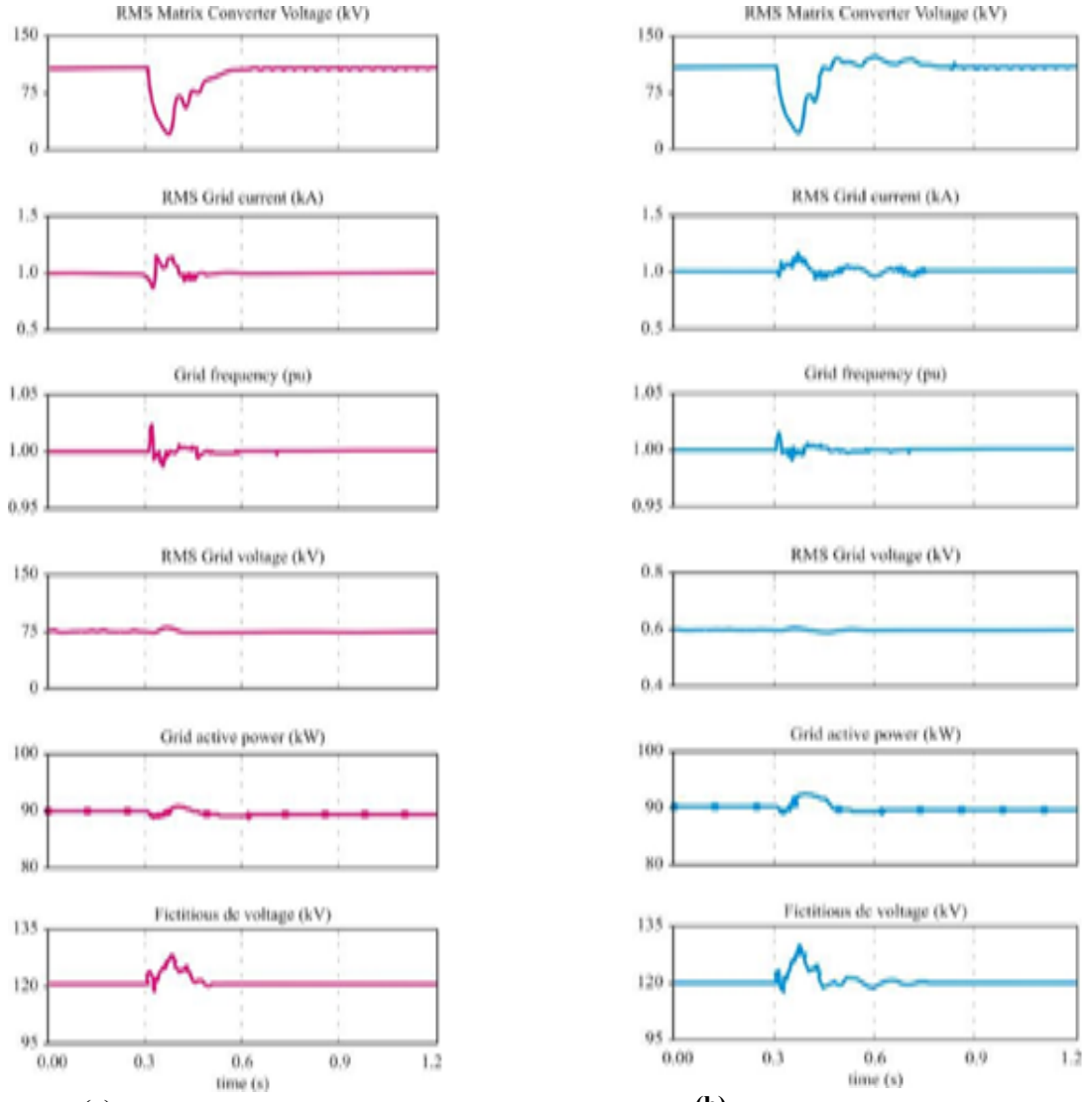

(a) With Proposed Control **(b) Without Proposed Control**

Fig. 8.12 Simulated Response of the Proposed MC Interfaced WECS under Three-Phase Fault with (a) Proposed Control (b) Conventional control (Where Waveforms are of RMS Matrix Converter Voltage, RMS grid Current, Grid Frequency, Grid Voltage, Grid Active Power, and Fictitious DC Link Voltage)

The ideal blocking period for serious faults, which is 0.2 milliseconds for single phase faults and 15 seconds for three phase faults, is monitored by the newly developed fuzzy control system. As seen in Fig. 33, when the system is simulating winds of 10 m/s, after a malfunction the grid voltage fully recovers in 0.5 seconds without triggering the trip of the wind turbine. Figure 33 demonstrates that applying the advised strategy yields a negligible improvement in transient stability. The issue barely affects the grid frequency in the wind turbine in addition to the continuous grid voltage.

Tiny voltage drops recover in 0.35 seconds when using the suggested method, which complies with grid code requirements. The system's overall response is therefore more tolerable and less fluctuating with improved performance characteristics when Fuzzy logic control and MMC are used as the control technique to reduce unneeded fluctuations and improve stability.

8.3 Simulation Results of Various Parameter under Varying Load Conditions

In this case, the load alternates between a bigger and a lower number. Through simulation, the dynamic functionality of WECS with MMC interfaced DFIG was tested. As in the situations above, Fig. 8.13 displays the frequency, modulation index, fictions DC link voltage, load voltage, generator voltage, load current, and load voltage for both control techniques. The outcomes of both control systems are compared in this section for a range of load circumstances.

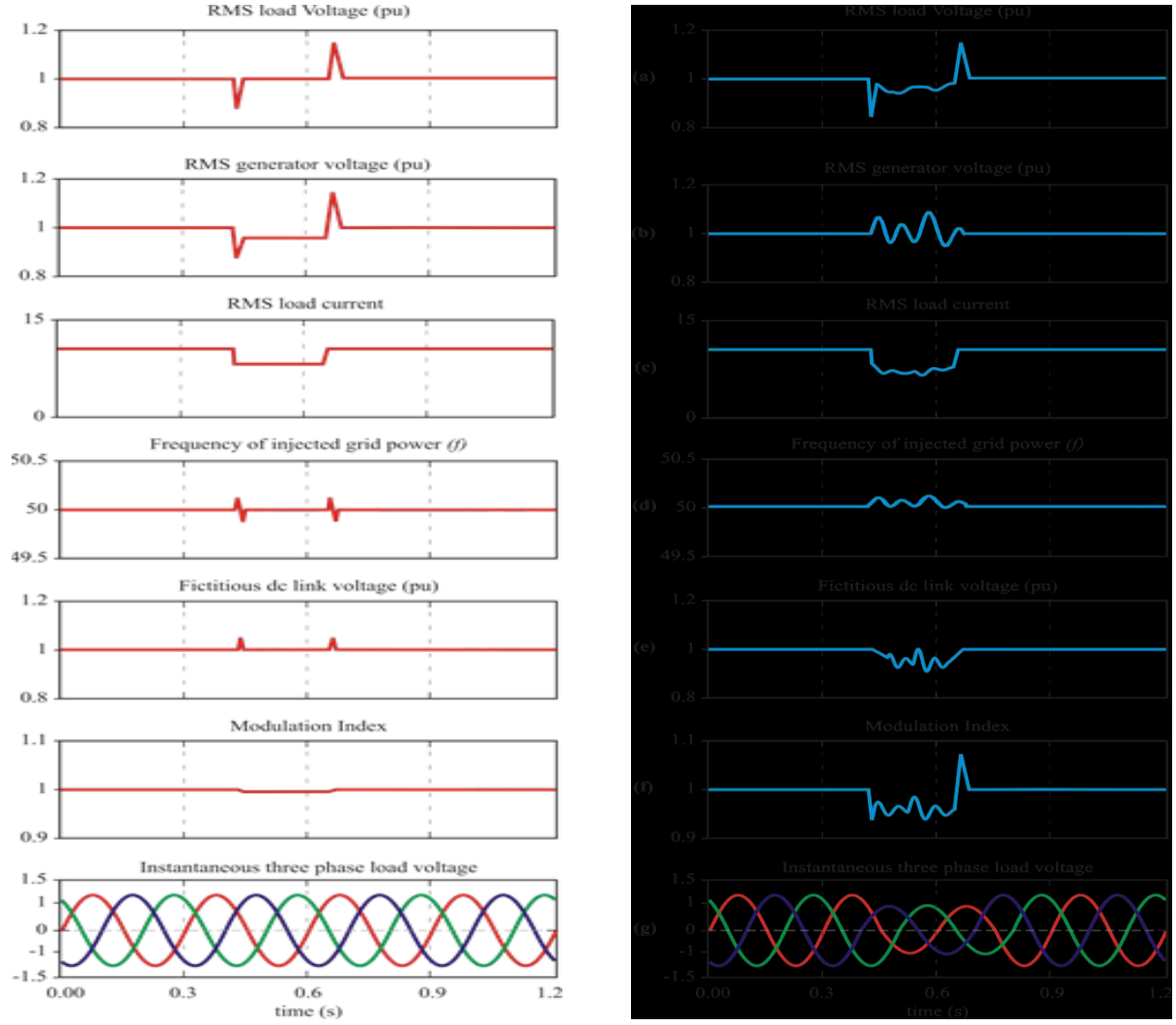

(a) With Proposed Control **(b) Without Proposed Control**

Fig. 8.13 Simulated Waveform during Varying Load Condition (A) Proposed Control (B) Conventional Control, (where (a) RMS Load Voltage, (b) RMS Generator Voltage; (c) RMS Load Current (d) Frequency (e) Fictitious DC Link Voltage (f) Modulation Index (g) Instantaneous Three Phase Grid Voltage

The load voltage is maintained constant by the controller when the load swings between half and full load, but when it fluctuates between full and half load, a control action is needed to maintain the load voltage's constant magnitude. In the first case, the load current is raised, whereas in the second, it is lowered.

In order to manage the load voltage during this process, the MMC's output current is maintained. With the help of the modulation index, the suggested control system can easily stabilize load voltage despite changing load conditions. As we contrast both conventional control and proposed control, the generated control techniques also evaluate the disturbance rejection capabilities. This demonstrates why the proposed control is better than conventional control as the latter cannot reduce any fluctuation caused by changes in load conditions.

CONCLUSION

In contrast to conventional PI controllers, a fuzzy logic controller approach is created for MMC-based DFIG in order to better meet performance requirements. These conclusions have been made: -

The multilevel matrix converter system's input filters reduced the effects of lower harmonic components. Harmonic balance has been achieved by reducing the ripple component of the input current and voltage waveforms. The control range of an FLC-based multilevel matrix converter is increased by the suggested method because it maintains a higher power factor at the input. A system that operates with a range of changeable parameters under balanced and unbalanced conditions with shifting loads can be given a complete steady state study using this technique. This steady state study also establishes the stability of the system and illustrates how different system variables affect stable responses. The

recommended controller is reliable under conditions of shifting loads and rotor speeds, as shown by simulation and experimental findings.

This control method improves efficacy by displaying a collection of output voltages that is balanced and has the required magnitude and frequency. Reduces balanced power harmonics, voltage harmonics, and current harmonics, as well as output power ripple. Rotor voltage restricts reactive power generation capability at lower rotor speeds, whereas rotor current limits it at higher rotor speeds.

Therefore, in this instance, the recommended control strategy improves the DFIG's reactive power capabilities. Additionally, this technique considerably supports grid voltage during times of reduced wind speed changes or short circuits. The outcomes of models and testing have proven that the DFIG has a consistent output voltage and current with little power loss.

REFERENCES

[1] Abad, G., Miguel A. angel Rodrıguez et al.: 'Direct Power Control of Doubly-Fed Induction Generator-Based Wind Turbines Under Unbalanced Grid Voltage IEEE Transactions on Power Electronics, 25(2), Feb. 2010, pp. 442-452.

[2] Abbey, C., et al.: 'Modeling Requirements for Transient Stability Studies for Wind Parks' IEEE Power Engineering Society General Meeting. Montreal, Que.,Canada, October 2006, pp:6-12

[3] Abdel-Baqi O. and Nasiri, A., 'A Dynamic LVRT Solution for Doubly-Fed Induction Generator Power Electronics and Electric Motor Drives Laboratory'.

[4] Baggu, M.M., Chowdhury, B.H,: 'Implementation of a Converter in Sequence Domain to Counter Voltage Imbalances. Power Engineering Society General Meeting held at Tampa, USA during 24-28 June 2007, pp.1-5.

[5] Baroudi, J. Dinavahi, A. V. and Knight, A. M. "A review of power converter topologies for wind generators," International Journal of Renewable Energy, 32(14), pp. 2369–2385, 2007.

[6] Barros, L.S., Mota, W.S. et al.: 'An Optimal Control Strategy for DFIG', IEEE International Conference on Industrial Technology, Vina del Mar, Chile, May 2010.

[7] Beltran, B., Mohamed El HachemiBenbouzid, et al.: 'Second Order Sliding Mode Control of a Doubly Fed Induction Generator Driven Wind Turbine', IEEE Transactions on Energy Conversion, 27 (2), June 2012, pp.: 261 - 269.

[8] Bhuiyan F.A., Yazdani, A.: 'Multimode Control of a DFIG-Based Wind-Power Unit for Remote Applications. Published in: IEEE Transactions on Power Delivery 24 (4), Oct. 2009, pp: 2079 – 2089.

[9] Blaabjerg, F. Liserre, M. and Ma, K. "Power electronics converters for wind turbine systems," IEEE Transactions on Industry Applications, 48(2), pp. 708–719, March 2012.

[10] Bourdoulis, M.K., Alexandridis, A.T,: 'An Alternative Modeling and Controller Design Guaranteeing Power Stability for DFIG Wind Systems', 52nd IEEE Conference on Decision and Control, Florence, Italy, March 2014.

[11] C. Klumpner, P. Nielsen, I. Boldea, F. Blaabjerg, A New Matrix Converter-Motor (MCM) for Industry Applications, Conference Record of the IEEE Industry Applications Society Annual Meeting, IEEE-IAS, 2000.

[12] Cai, L.J., Erlich, I., Karaagac, U., Mahseredjian, J,: 'Stable Operation of Doubly-fed Induction Generator in Weak Grids', IEEE Power & Energy Society General Meeting, Denver, CO, USA, July 2015.

[13] Calvillo, C. F., Martell, F., et al.: 'Rotor Current Fuzzy Control of a DFIG with an Indirect Matrix Converter'. 37th Annual Conference of the IEEE Industrial Electronics Society, Melbourne, VIC, Australia, January 2012.

[14] Calvillo', C. F., Olloqui, A. et al.: 'Comparison of Model Based Predictive Control and Fuzzy Logic Control of a DFIG with an Indirect Matrix Converter', 38th Annual Conference on IEEE Industrial Electronics Society, Montreal, QC, Canada, December 2012.

[15] Chen, S. Z., Cheung, N.C., et al.: 'Integral Sliding-Mode Direct Torque Control of Doubly-Fed Induction Generators Under Unbalanced Grid Voltage. Integral Sliding-Mode Direct Torque Control of Doubly-Fed Induction Generators under Unbalanced Grid Voltage', IEEE Transactions on Energy Conversion, 25 (2), June 2010, pp.: 356 – 368.

[16] Chen, Z. "Issues of Connecting Wind Farms into Power Systems", 05 IEEE/PES Transmission & Distribution Conference & Exposition: Asia and Pacific, Dalian, China, December 2005.

[17] Chen, Z., Hu, Y., and Blaabjerg, F.: 'Stability improvement of induction generator-based wind turbine systems', IET Renew. Power Gener., 2007, 1(1), pp. 81–93.

[18] Forchetti D., Garcia G., and M.I. Valla, „Vector control strategy for a doubly-fed stand-alone induction generator", Proc. IEEE 28th Annual Conf. of the Industrial Electronics Society, 2, Nov. 2002, pp. 991 – 995.

[19] Datta R., Ranganathan, V.T, 'Decoupled control of active and reactive power for a Grid-Connected Doubly-Fed Wound Rotor Induction Machine without position sensors' IEEE Industry Applications Conference. Thirty-Fourth IAS Annual Meeting (Cat. No.99CH36370), Phoenix, AZ, USA, USA, pp.:

[20] Deshmukh, M.K., Moorthy, C. B.: 'Review on Stability Analysis of Grid Connected Wind Power Generating System International Journal of Engineering Research and Development (IJEEERD)', 3(1), (2013), pp. 01-33.

[21] Dhar B.: "PhD. thesis Study of Stability Analysis of a Grid-Connected Doubly Fed Induction Generator (DFIG)-based small Wind Farm", The University of Western Ontario.
[22] Diaz M., Rojas F. Control of Modular Multilevel Cascade Converters for Offshore Wind Energy Generation and Transmission, Thirteenth International Conference on Ecological Vehicles and Renewable Energies (EVER) Monaco, 2018.
[23] Duarte, J.L., A. Van Zwam. et al.: 'Reference frames fit for controlling PWM rectifiers' IEEE Transactions on Industrial Electronics. 46, (3) Jun 1999 pp.:628- 630.
[24] Earnest, J. and Wizelius, T. Wind Power Plants and Project Development. New Delhi, India: PHI Learning May 2011.
[25] Ekanayake, J. and Jenkins, N. "Comparison of the response of doubly fed and fixed speed induction generator wind turbines to changes in network frequency," IEEE Transactions on Energy Conversion, 19(4), pp. 800–802, December 2004.
[26] Feltes, C., Wrede, H., Koch F. W., and Erlich, I. 'Enhanced Fault Ride-Through Method for Wind Farms Connected to the Grid Through VSC-Based HVDC Transmission', IEEE Transactions on Power Systems, August 2009, 24(4), pp.1537-1546.
[27] Franco, R., Capovilla, C. E. et al.: 'A deadbeat direct power control applied to doubly fed induction aerogenerator under normal and sag voltages conditions', 40th Annual Conference of the IEEE Industrial Electronics Society, Dallas, TX, USA, February 2015
[28] Fung, K. T., Scheffler R. L.; Stolpe J. Wind Energy - A Utility Perspective Published in: IEEE Transactions on Power Apparatus and Systems PAS100, 3 March 1981, pp : 1176 – 1182.
[29] Ghoshand, S., Kamalasadan, S,: 'An Integrated Dynamic Modeling and Adaptive Controller Approach for Flywheel Augmented DFIG Based Wind System' IEEE Transactions on Power Systems, 32 (3), May 2017, pp. 2161 - 2171.
[30] Gomis-Bellmunt, O., Adri`aJunyent-Ferr´e, Andreas Sumper and Joan Bergas-Jan´e,: 'Ride Through Control of a Doubly Fed Induction Generator Under Unbalanced Voltage Sags", IEEE Transactions on Energy Conversion, December 2008, 23(4), pp.: 1036 – 1045.
[31] Gong, B., Xu, D., Wu, B,: 'Cost Effective Method for DFIG Fault Ride-through During Symmetrical Voltage Dip'. Graham Pannell, David J. Atkinson, And Bashar Zahawi,"Minimum-Threshold Crowbar For Afault-Ride-Through Grid-Code-Compliant DFIG Wind Turbine", IEEE Transactions On Energy Conversion, 25(3), September 2010.
[32] Guofeng,Y., Yongdong, L., et al.: „A Novel Position Sensor-less Control Scheme of Doubly Fed Induction Wind Generator Based on MRAS Method". IEEE Power Electronics Specialists Conference, Rhodes, Greece, June 2008. pp.167-172.
[33] H. Huang, Y. Fan, R.C. Qiu, and X.D. Jiang, "Quasi-steady-state rotor EMF-oriented vector control of doubly fed winding induction generators for wind-energy generation", Electric Power Components and Systems, 34(11), Nov. 2006, pp. 1201-1211.
[34] Hamane, B., Doumbia, M. L,: 'Direct Active and Reactive Power Control of DFIG based WECS using PI and Sliding Mode Controllers'40th Annual Conference of the IEEE Industrial Electronics Society., Dallas, TX, USA, February 2015.
[35] Hany M. Jabr and Narayan C. Kar, "Fuzzy Gain Tuner for Vector Control of DoublyFed Wind Driven Induction Generator. Published in: 2006 Canadian Conference on Electrical and Computer Engineering, Ottawa, Ont., Canada, Jan. 2007.